Research Square

Preprints are preliminary reports that have not undergone peer review.
They should not be considered conclusive, used to inform clinical practice,
or referenced by the media as validated information.

Polydopamine-based Polysaccharide Materials for Water Treatment

Fangfei Liu
Xinjiang University
Ruxangul Jamal
Xinjiang University
Tursun Abdiryim
Xinjiang University
Xiong Liu (liuxiong.1991@qq.com)
Xinjiang University https://orcid.org/0000-0002-7113-2313

Research Article

Keywords: polysaccharide, polydopamine, adsorption, oil-water separation, catalysis, solar-driven water purification

Posted Date: June 23rd, 2022

DOI: https://doi.org/10.21203/rs.3.rs-1712970/v1

License: This work is licensed under a Creative Commons Attribution 4.0 International License.
Read Full License

Abstract

Low-cost polysaccharides, such as cellulose, chitosan, chitin and alginate, have come into people's sight for water treatment. Nevertheless, their treatment efficiency and capability are sometimes unsatisfactory because of the lack of active sites and functionalities. In recent years, more and more attentions have been paid to the integration of polydopamine (PDA) into polysaccharide-based materials to develop high-performance products for wastewater treatment. PDA modification can endow polysaccharides with plentiful functional moieties (including catechol, amine, and phenyl groups) for binding heavy metals and organic pollutants. PDA coatings may increase interfacial stability and hydrophilicity for oil/water separation. PDA also may anchor various catalysts for catalytic degradation of organic pollutants. Furthermore, the good light-harvesting capability and photothermal transformation feature of PDA are available for solar-driven water purification. This review aims to give the comprehensive overview on the development of PDA-based polysaccharide materials for water treatment. PDA-based polysaccharide materials can be made into cost-effective and high-performance products (including hydrogels, aerogels, membrane, beads and nanocomposites) for adsorption of heavy metals and organic pollutants, oil/water separation, catalytic degradation of organic pollutants, and solar-driven water purification. This review will give a valuable information for the design and exploitation of PDA-based polysaccharide materials in water treatment.

1. Introduction

With the intensification of agricultural and industrial activities, various contaminations including heavy metals, chemical dyes, spilled oils and other organic aromatic pollutants are gradually accumulating in water, leading to the potential hazardous effects on human health (Gusain et al. 2020; Schwarzenbach et al. 2010). There is no denying the fact that the water pollution is a pretty serious problem, hence great efforts should be paid to deal with it. Based on the present severe situation, researchers have devoted diverse efforts to solve the water pollution problems. Traditional materials (such as activated carbons) used in process of water treatment are expensive and energy intensive, and may rack up a huge carbon footprint (Crini et al. 2019; Thompson et al. 2016). Therefore, it will be very important to exploit cut-price, eco-friendly alternatives with outstanding properties and lower carbon footprint for meeting the requirement of sustainable development. In this context, green and sustainable materials have raised widespread attention in water treatment processes.

Polysaccharides, such as cellulose, chitin, chitosan and alginate, which are common, easy-gained, biodegradable, renewable and low-cost begin to come into people's sight for water treatment (Gandini et al. 2016). Polysaccharides with green and sustainable characteristics have been considered as available alternatives to synthetic polymers, and have the potential values for both research and commercial applications (Avcu et al. 2019). With the abundant functional groups including -OH, -COOH, and -NH_2, polysaccharides have shown the huge advantages for water treatment. For example, cellulose containing many -OH group is able to adsorb cations, chitin/chitosan containing -NH_2 group has the advantage for adsorbing anions, and alginate containing -COOH group prefers to remove heavy metal ions

(Nasrollahzadeh et al. 2021). Polysaccharides are also made into various products (including hydrogels, aerogels, membrane, beads, and nanocomposites) for oil/water separation, as well as to support catalysts for catalytic degradation of organic pollutants (Chen et al. 2021a; Dong et al. 2021). However, the efficiency and capability of these natural polysaccharides are sometimes limited because of the insufficient functional groups reacted with contaminants and bad wettability. Therefore, there has been a growing interest for modifying polysaccharides to endow them with some preferred performances and functionalities. Conventional chemical modification strategies involve esterification, etherification, halogenation, oxidation, carboxymethylation, acetylation, polymer grafts, phosphorylation, sulfation and so on, which provides a good pathway to tailor their surface charges, compositions, roughness and functionalities (Caputo et al. 2019; Messina et al. 2020). Although these methods can obtain high degree of modification, they often perform tedious operation, long reaction time, high energy consumption, secondary pollution, harsh reaction conditions, and side reactions (Laureano-Anzaldo et al. 2021). Thus, it is urgent to exploit new modification approaches for overcoming most of the above disadvantages to realize high efficiency and minimal environmental impact.

Inspired by marine mussels, in 2007, Messersmith et al. (Lee et al. 2007) observed that dopamine had a fascinating advantage: the ability to generate PDA via a self-polymerization process, and PDA could serve as a strong coating material because of its surface-independent deposition performance and long-term stability. Since then, PDA has been widely applied for surface modification of all kinds of inorganic and organic materials based on its versatility, simplicity and high efficiency, and a mass of excellent reviews have been reported for dopamine chemistry (Lee et al. 2020; Liu et al. 2014; Patil et al. 2018; Zhang et al. 2020a; Zhang et al. 2020b). According to research findings, PDA has several obvious advantages. First, PDA possesses plentiful functional moieties (including catechol, amine, and phenyl groups), which contribute to binding metals and organic molecules through electrostatic, coordinate, chelate, H-bonding, and π-π stacking interactions (Xie et al. 2020). Second, PDA can act as a universal surface modification agent. Third, PDA has good light-harvesting capability and photothermal transformation feature (Liu et al. 2013). Fourth, PDA might readily react with amine- or thiolate-functionalized compounds through Michael addition or Schiff base reactions to prepare multifunctional hybrid materials. Based on its characteristic properties, PDA has shown a variety of promising applications such as heavy metals and organic pollutants removal (Sun et al. 2018), oil/water separation (Nayak et al. 2021), sea water desalination (Chaule et al. 2021), supercapacitors (Yang et al. 2021), catalysts (Zhou et al. 2014), self-healing materials (Wang et al. 2019), drug delivery (Du et al. 2021), wound dressing (Tao et al. 2020) and so on.

In recent years, more and more attentions have been paid to the integration of PDA into polysaccharide-based materials (especially low-cost polysaccharides, mainly including cellulose, chitosan, chitin and alginate) to develop all kinds of cost-effective and high-performance products (such as hydrogels, aerogels, membrane, beads, nanocomposites, and so on) for water treatment. And research on this new PDA-based polysaccharide materials has developed rapidly, as can also be seen in the growing number of publications. This review aims to give a comprehensive overview on the development of PDA-based polysaccharide materials for environmental applications including adsorption of heavy metals and

organic pollutants, oil/water separation, catalytic degradation of organic pollutants, as well as solar-driven water purification (Fig. 1). This review is expected to give a guideline for the emerging field and offers new inspirations for the design and development of PDA-based polysaccharide materials for water treatment.

2. Polydopamine Structure And Formation

PDA originated in a groundbreaking discovery that dopamine monomer was subjected to a self-polymerization process in moderate conditions to generate the polymeric structures of PDA (Lee et al. 2007). This work was mostly inspired from the wet adhesion proteins (generated from mussels) that adhere to a variety of inorganic and organic surfaces, in which the cooccurrence of catechol and amine moieties was identified as the chief cause of tough adhesion. Although PDA has been used so much today, its formation mechanism is still unclear. It is a huge challenge to make sense of the PDA formation process, and its mechanism analysis maintain a highly active state. In a commonly accepted route, dopamine monomer is first oxidized to form a dopamine-quinone intermediate that is then subjected to a nucleophilic intramolecular cyclization process to generate leukodopaminechrome, followed by the oxidation and rearrangement to produce 5,6-dihydroxyindole or 5,6-indolequinone (Fig. 2) (Della Vecchia et al. 2013; Ponzio et al. 2016). In this way, the different manners are proposed to form the ultimate PDA structure and illustrate formation mechanism. The possible mechanism involves the intermolecular crosslink of 5,6-dihydroxyindole or 5,6-indolequinone via branching reaction pathways, resulting in the melanin-like PDA structure. And, it is worth noting that a mass of uncyclized oxidized dopamine containing primary amine moieties can react intermolecularly with either 5,6-dihydroxyindole or dopamine through catechol-to-catechol coupling, leading to the diverse structure of PDA. In another way, dopamine molecule loses a single electron to form a dopamine-semiquinone radical under light-irradiation (Du et al. 2014). Whereafter, the radical intermediate is either oxidized into the dopamine-quinone or undergoes the intermolecular coupling to generate a catechol-to-catechol dimer. It has been proved that the catechol-to-catechol coupling process is successfully applied for the PDA-based surface functionalization (Yang et al. 2021). In addition, the non-covalent self-assembly route also can form PDA. All kinds of intermolecular interactions, such as π-π stacking, H-bonding, cation-π, quadrupole-quadrupole, T-shape and ionic interactions, help to induce PDA formation (Hong et al. 2018). Despite the intricate formation mechanisms, PDA is able to take part in a variety of interfacial interactions including π-π stacking, cation − π, H-bonding, metal coordination, borate complexation, redox, Michael addition, Schiff-base reaction and catechol-quinone conjugation (Fig. 2), which provides a simple, versatile and forceful platform for the material-independent surface modification and the preparation of various functional hybrid materials to realize broad applications.

3. Polydopamine-based Polysaccharide Materials For Water Treatment

3.1. Adsorption of heavy metals and organic pollutants

Adsorption is regarded as a comparatively simple and efficient approach for removing heavy metals and organic pollutants in wastewater treatment (Krasucka et al. 2021; Pan et al. 2021). Adsorption mechanisms are commonly attributed to physicochemical interactions between adsorbates and absorbents, including electrostatic interactions, ion exchange, metal chelation or complexation. In order to decrease the environmental effect in the adsorption processes, desired absorbent materials should possess some necessary features, such as high-efficiency, renewability, environmental protection, as well as rich source. In addition, absorbent materials should demand minimal processing before use. Biomass-based absorbents give a significant contribution to realize above goals. Polysaccharides with renewability, biodegradability, low cost and biocompatibility have been regarded as the promising candidates for the preparation of all kinds of high-efficiency absorbents. However, their adsorption efficiency is sometimes unsatisfactory due to the lack of active adsorption sites. PDA with abundant active groups (such as catechol, amine, and phenyl units) results in the formation of multiple interactions (such as electrostatic, coordinate, chelate, H-bonding, and π-π stacking interactions) with heavy metals and organic pollutants, resulting in the enhanced adsorption efficiency of adsorbents. In this following section, the use of PDA-modified polysaccharide materials as adsorbents for removing heavy metals and organic pollutants will be highlighted. In general, PDA can endow polysaccharides with additional reactive functional groups, thus improving their adsorption capacity. Table 1 shows the summary descriptions of PDA-based polysaccharide materials for adsorbing heavy metals and organic pollutants.

Table 1
PDA-based polysaccharide materials for adsorbing heavy metals and organic pollutants.

Compositions	Adsorption capacity	Ref.
CNFs, PDA, PEI	Cu(II): 103.5 mg g^{-1}; MO: 265.9 mg g^{-1}	(Tang et al. 2019)
CNCs, PDA	Cr(VI): 205.0 mg g^{-1}	(Dong et al. 2019)
CNCs, PDA	MB: 2066.7 mg g^{-1}	(Wang et al. 2020b)
CNCs, PDA	MB: 130.0 mg g^{-1}	(Mohammed et al. 2021)
Microcrystalline cellulose, PDA	MB: 153.4 mg g^{-1}	(Wei et al. 2018)
BC, PDA, MOFs	U(VI): 535.0 mg g^{-1}	(Zhou, et al. 2021)
Cellulose, PDA, MXene	MB: 168.9 mg g^{-1}	(Zhang et al. 2021)
Cellulose, PDA, Fe_3O_4	Resorcinol: 258.0 mg g^{-1}	(Ding et al. 2017)
Cellulose acetate butyrate, PDA	Caffeine: 40%	(Furtado et al. 2020)
Cellulose acetate, PDA	MB: 69.89 mg g^{-1}; CR: 67.3 mg g^{-1}	(Chen, et al. 2020)
Lanthanum-chitosan, PDA	Phosphate: 195.3 mg g^{-1}	(Zhao et al. 2020)
Carboxyl methylcellulose, chitosan, PDA, PEI	Cd(II): 470.0 mg g^{-1}; Cr(VI): 370.0 mg g^{-1}	(Li et al. 2020)
Chitosan, PDA, poly (L-lactic acid)	Cu(II): 270.2 mg g^{-1}	(Zia et al. 2021)
Calcium alginate, chitosan, PDA	Difenoconazole: 66.5%; nitenpyram: 51.3%	(Zhou et al. 2022)
Carboxymethyl chitosan, PDA, carbon nanotubes	Cu(II): 38.2 mg g^{-1}	(Zeng et al. 2016)
Chitosan, PDA, Fe_3O_4	Hg(II): 245.6 mg g^{-1}; Pb(II): 47.0 mg g^{-1}; Cr(VI): 151.6 mg g^{-1}; MB: 204.0 mg g^{-1}; malachite green: 61 mg g^{-1}	(Wang et al. 2016)
Chitosan, PDA, magnetic fly ash	Ag(I): 57.0 mg g^{-1}	(Mu et al. 2020)

Compositions	Adsorption capacity	Ref.
Chitosan, PDA	Cr(VI): 374.4 mg g^{-1}; Pb(II): 441.2 mg g^{-1}	(Guo et al. 2018)
Chitosan, PDA, GO	U(VI): 415.9 mg g^{-1}	(Liao et al. 2018b)
Chitosan, PDA, GO	Cr(VI): 312.0 mg g^{-1}	(Li et al. 2020)
Chitosan, PDA, MWCNTs, GO	Gd(III): 150.86 mg g^{-1}	(Zhang et al. 2021)
Chitosan, PDA, attapulgite	U(VI): 175.1 mg g^{-1}	(Liao et al. 2018a)
Sodium alginate, PDA, $CoFe_2O_4$	MB: 466.6 mg g^{-1}; CV: 456.52 mg g^{-1}	(Li et al. 2016)
Sodium alginate, PDA, PEI, $CaCO_3$	Cr(VI): 524.7 mg g^{-1}	(Yan et al. 2017)
Sodium alginate, PDA, γ-Fe_2O_3	Thorium: 326.3 mg g^{-1}	(Ding et al. 2019)
Calcium alginate, PDA, Al-pillared montmorillonite	As(V): 61.9 mg g^{-1}	(Song et al. 2019)

Cellulose, as the most abundant renewable resource on our planet, is biodegradable, biocompatible and non-toxic, and possesses a great number of modifiable hydroxyl groups. The characteristic properties of cellulose and its derivatives (such as cellulose nanofibrils (CNFs), cellulose nanocrystals (CNCs) and bacterial cellulose (BC)), including large surface area, high aspect ratio, remarkable surface functionalization possibility, high mechanical strength and large-scale availability endow them potential applications in adsorbing heavy metals and organic pollutants (Mahfoudhi and Boufi 2017). However, pristine cellulose generally exhibited very limited adsorption ability. In order to increase adsorption ability of cellulose, various surface modification strategies have been developed. PDA-based surface modification methods have become facile and effective strategies to endow cellulose with acceptable adsorption ability. Currently, PDA-functionalized cellulose or cellulose derivative materials have the ability to become low-cost, bio-renewable and efficient materials for applications in the efficient adsorption of heavy metals and organic pollutants. For example, CNFs could be functionalized via PDA to prepare all kinds of cost-effective adsorption materials for removing heavy metals and organic pollutants. Tam et al. (Tang et al. 2019) used PDA to coat CNF surface, resulting in the compressible CNF-based aerogels that could be used for removing heavy metal ions and dyes. As shown in Fig. 3a, PDA was first introduced to the surface of CNF at pH 8.0 by the self-polymerization of dopamine, and then polyethylenimine (PEI) was employed to cross-link the PDA-coated CNF (PDA-CNF), leading to the formation of the PDA-CNF-PEI aerogels. The possible crosslinked mechanism between PDA-CNF and PEI was that the active groups of

PDA-CNF might react with PEI through Michael-addition or Schiff-base reactions (Fig. 3b). As a result, the PDA-CNF-PEI aerogels had a low density (25.0 mg/cm^3), high porosity (98.5%) and shape recovery in air and water, indicating that the obtained aerogels were stable and robust. Due to the PDA coatings, the PDA-CNF-PEI aerogels possessed a great number of active sites. So, the aerogels could be applied as effective adsorbing materials for removing metal ions or dyes. Adsorption experiments demonstrated that PDA-CNF-PEI aerogels displayed a maximum adsorption ability of 103.5 mg g^{-1} for Cu(II) and 265.9 mg g^{-1} for methyl orange (MO), respectively. It was also found that the pH values have an impact on the adsorption process, because the responsive behavior of PDA and PEI could be affected by the acidity and alkalinity of solution (Fig. 3c). Recycling experiment proved that PDA-CNF-PEI aerogels could be used as a regenerated adsorbent. In detail, Cu(II) or MO loaded adsorbents were able to be readily reused at least four times with the efficiency up to 91% or 89%. The low-cost, excellent adsorption capacity and efficiency of PDA-CNF-PEI aerogel has a promising future in wastewater treatments. By specifically tuning the surface of the CNFs, its selectivity and adsorption capacity for heavy metals could be improved. Chang's group (Dwivedi et al. 2017) reported that dopamine was first conjugated to CNFs, followed by the crosslinking with Fe^{3+} to generate Fe-containing dopamine-grafted CNFs that showed high absorption capacity for As(V) (19.85 mg g^{-1}) and Cr(VI) (25.95 mg g^{-1}). What's more, the as-prepared Fe-containing dopamine-grafted CNFs could reduce harmful Cr(VI) to nontoxic Cr(III).

Like CNFs, CNCs are also often used to prepare adsorption materials. A CNC-based adsorbent was prepared via the efficient PDA-based surface modification, showing remarkable Cr(VI) adsorption ability (Dong et al. 2019). The nanoadsorbents were prepared by coating PDA onto the acid-hydrolyzed cellulose in the buffer solution, as shown in Fig. 4a. By adjusting the polymerization of dopamine on CNC surface, PDA-functionalized CNC (CNC@PDA) was obtained. In CNC@PDA, PDA nanoparticles with less than 30 nm uniformly distributed to the surface of CNCs. The particular hierarchical structure endowed the resulting CNC@PDA with good adsorbing capacity towards Cr(VI) (205 mg g^{-1}). And its adsorption performance was better than most cellulose-base adsorbents. Interestingly, the CNC@PDA nanoadsorbents could be easily recycled without complicated separation procedures because dense flocs were immediately formed and precipitated out from the solution after mixing the adsorbents and Cr(VI) (Fig. 4b and 4c), which was significant for reclaiming the purified water without complicated separation. The mussel-inspired approach to prepare nanocomposites with these special hierarchical structures may offer a chance for the application of cellulose-containing agriculture by-products in wastewater treatment field. Nanocomposites prepared by CNCs and PDA exhibited an obvious core–shell architecture (specific surface area: 107.2 m^2 g^{-1}; maximum MB adsorption ability: 2066.72 mg g^{-1}), and showed good recyclability for four adsorption-regeneration cycles (Wang et al. 2020b). Recently, PDA-functionalized CNCs were reported to selectively adsorb methylene blue (MB), (100%) and partially remove MO (50.02%) in a MB/MO mixture system (Fig. 4d) (Mohammed et al. 2021). In these adsorption studies of the binary mixture systems (such as MB/MO, MB/rhodamine B (RhB), and MB/crystal violet (CV)), it was found that the enhanced selectivity of the PDA-functionalized CNCs for MB was on account of the synergistic interactions including electrostatic attraction, π-π stacking, and H-bonding between PDA and MB.

Improving the adsorption capacity of one contaminant is obviously not enough in single component system, because other components can also largely influence the adsorption capacity in practical application. A PDA-microcrystalline cellulose aerogel with good adsorption ability towards dyes was obtained via the self-polymerization of dopamine in the solution of microcrystalline cellulose and LiBr, followed by a freeze-dried strategy (Wei et al. 2018). The structure stability of aerogels networks was also improved by introducing PDA. The adsorption quantity of aerogels increased with the increasing PDA content, and the maximum adsorption efficiency of this kind of aerogels toward MB reached up to 94.4%. In addition, the maximum adsorption capacity is around 153.4 mg g^{-1}. More importantly, the aerogel showed good adsorption selectivity toward MB in different mixed solution. In both mixed solutions of MB/safranine T (ST) and MB/RB, the removal rate of MB was still-high (96%), but the removal rates toward ST and RhB were merely 37% and 21%, respectively. And, the resulting aerogel also had high efficiency to remove MB in high NaCl concentrations. It is believed that this composite aerogel with high adsorption efficiency and remarkable adsorption selectivity will have greatly potential applications in wastewater treatment.

PDA is also introduced into culture medium during the growth of BC, which is thought as a cost-effective and flexible method to fabricate functional PDA-based cellulose materials for sustainable water treatment. A robust PDA particles/bacterial nanocellulose (BNC) composite film was reported for high-efficiency removal of Pb(II), Cd(II), rhodamine 6G (R6G), MB, and MO (Derami et al. 2019). In order to obtain PDA particles, dopamine monomer was self-polymerized with the help of oxygen in a mixture solution of water, ethanol and ammonium. In this process, the sizes of PDA nanoparticles may be controlled by changing influence factors, such as the concentration of ammonium. To immobilize the particles in the network of BNC during the operational conditions, the diameters of PDA particles were adjusted to around 800 nm. PDA particles with highly uniform diameter were mixed with bacterial culture and growth solutions, resulting in formation of the PDA/BNC hydrogel layer, and then the resulting hydrogel were air-dried to give a thin and dense PDA/BNC membrane. SEM measurement indicated that PDA particles were evenly distributed inside the BNC fiber network in both the hydrogel and the membrane. Subsequently, the obtained filtration film was used to continuously and rapidly remove organic dyes and heavy metal ions. For heavy metal pollutants, the PDA/BNC membrane had high efficiencies for removing both Pb(II) and Cd(II), while exhibiting better property in removing Pb(II). For organic pollutants, the filtration performance for both R6G and MB was found to be obviously higher than MO, indicating that the PDA/BNC membrane was not appropriate for the removal of negatively charged pollutants. In addition, the film not only exhibited outstanding aqueous stability and fast water transport, but also was effective for the removing of single or multiple pollutants. More importantly, it was very convenient to regenerate and reuse the films for several times after simple washing with regeneration agents, and its adsorption capacity and mechanical integrity had no significant degradation. The novel water treatment film with remarkable mechanical robustness will be a hopeful candidate for sewage treatment.

A similar approach was also adopted to prepare the biocompatible PDA/BC composite with hierarchical structure for enzyme immobilization to degrade dyes in wastewater treatment process (Zhai et al. 2019). The composite was fabricated by a simple strategy, in which BC was immersed in dopamine aqueous solution (pH > 7), leading to *in-situ* formation of PDA nanoparticles on cellulose surface. The resulting hybrid composite showed super enzyme immobilization efficiency of ca. 165 mg g^{-1}. Compared to the free laccase, the immobilized laccase presented better thermostability and operational stability over a wide temperature range. In the dye decolorization test, the obtained PDA/BNC/laccase composite exhibited excellent dye removal property and recyclability, which indicated its promising application in the wastewater treatment.

The combination of PDA-functionalized BC and metal–organic frameworks (MOFs, high specific surface area and hydrothermal stability) (Wang and Astruc 2020) was applied to fabricate carbon aerogels with high specific surface area (220.45 m^2 g^{-1}) (Zhou et al. 2021). The carbon aerogels showed the maximum adsorption ability (535 mg g^{-1}) for U(VI) with good selectivity. Adsorption kinetic analysis indicated that the adsorption equilibrium could be reached within 70 min. And, the carbon aerogels still maintained 76% of the adsorption ability after five adsorption-regeneration cycles.

By introducing $Ti_3C_2T_x$ (MXene, a novel type of 2D material with high specific surface area, adjustable multilayer architecture, fine hydrophilic surface and remarkable stability) (Zhang et al. 2020) into PDA-functionalized cellulose aerogel, a high-performance adsorbent was obtained for removing MB (Fig. 5) (Zhang et al. 2021). The resulting composite aerogel had the specific surface area of 38.43 m^2 g^{-1} and showed the maximum adsorption ability of 168.93 mg g^{-1} for MB. Furthermore, it was observed that high concentration of Cl^- ion (over 3%) contributed to removing MB based on the adsorption behaviors in the existence of various salts (such as NaCl, $CaCl_2$, Na_2SO_4 and $CaSO_4$). The adsorption mechanism was considered to be the synergistic interactions including electrostatic attraction, π-π stacking, and H-bonding. This composite aerogel gives a chance to remove MB in high-salt conditions. By using the magnetic PDA to functionalize cellulose, a magnetic adsorption material was prepared to have high adsorption capacity to remove resorcinol from wastewater (Ding et al. 2017). This magnetic material showed better resorcinol removal capacity at low pH. It was also found that this material exhibited good durability and easy regeneration, and its adsorption capacity strongly relied on their surface charge concentration and specific surface area. This work provides good insights for phenols removal using magnetic composites in the future. PDA-functionalized cellulose acetate butyrate microbeads were used to remove caffeine (40%) (Furtado et al. 2020). Density functional theory (DFT) calculations indicated that the adsorption mechanism may be due to the synergistic interactions (including π-π stacking and H-bonding) between PDA and caffeine.

Nanofiltration membranes have been considered as a sort of excellent and efficient semi-permeable membranes for deeply purifying drinking water because of its low osmotic pressure and selective rejection of divalent salt ions (such as Ca^{2+}, Cu^{2+} and Mg^{2+}) (Lau et al. 2015). To obtain effective nanofiltration membrane, Huang and co-workers (Wang et al. 2020a) used the PDA to functionalize

regenerated cellulose membrane (RCM) followed by the interfacial polymerization of 1,3,5-trimesoyl chloride (TMC) and piperazine (PIP). PDA was conducive to binding the supporting layer of RCM through noncovalent interactions (such as H-bond, electrostatic interaction, and π-π stacking) and the active layer of polyamide through Michael addition. The as-prepared PDA-functionalized cellulose-based nanofiltration membrane possessed a three-layer structure with obviously increased stability (36 h). The obtained nanofiltration membrane had the rejection rates of 74.8% for Na_2SO_4, 66.3% for $MgSO_4$, 38.1% for NaCl, 27.1% for $MgCl_2$ and 26.7% for $CaCl_2$, respectively, and 90.2% for 4 kinds of dyes (MB, CV, CR and MO). Furthermore, the nanofiltration membrane possessed water-flux of 25.06 L m^{-2} h^{-1} under a 0.4 MPa pressure. This work presents a cost-effective way to fabricate biodegradable nanofiltration membrane for potential application in the purification of drinking water. To efficiently and synchronously adsorb cationic and anionic dyes, the electrospinning of cellulose acetate was combined with deacetylation, carboxymethylation and PDA surface modification to prepare cost-effective multifunctional membrane (Chen et al. 2020). The introduction of -COOH, -OH and -NH_2 groups into the fibers membrane resulted in the enhanced maximum adsorption abilities of 69.89 mg g^{-1} for MB and 67.31mg g^{-1} for Congo red (CR). Interestingly, the selective adsorption of MB and CR in a mixed system was accomplished through changing the degree of acidity or alkalinity of the solution. The high adsorption ability for MB was obtained at pH values of 3, 7 and 11, while the adsorption ability for CR was higher at pH values of 7 and 11 than the one at pH value 3. In addition, the multifunctional membrane also showed good stability and recyclability (five cycles).

Chitosan is generally prepared via the deacetylation of chitin that is second only to cellulose in the amount produced annually via biosynthesis, mainly from animals, existing in crustacean shells including shrimps, prawns, crabs and lobsters, in insects such as beetles, in cuttlefish of bone, in fungi such as mushrooms (Pillai et al. 2009). Due to the characteristic advantages of nontoxicity, biocompatibility, biodegradability, solubility, good reactivity, low cost, abundant in nature and desirable adsorption capability, chitosan is widely applied in water treatment, specifically in the removal of heavy metal ions and organic pollutants. The novel functional groups are introduced into chitosan, which will improve the density of sorption sites, change the pH range for metal sorption and vary the sorption sites for purpose of increasing sorption selectivity for the target metal ions (Alves and Mano 2008). The use of PDA to modify chitosan can prepare new and suitable biosorbents for heavy metal ions and organic pollutants.

To obtain cost-effective biomass-based adsorbents, PDA was applied to functionalize lanthanum-chitosan hydrogel (La-CS) (Fig. 6a) (Zhao et al. 2020). The doping lanthanum made the chitosan hydrogel more stable internal architecture and more precise selectivity, while the PDA coating provided additional reactive groups and reinforced the toughness of the chitosan hydrogel. The resulting La-CS@PDA showed a maximum adsorption ability of 195.3 mg g^{-1} for phosphate removal. In addition, the hydrogel adsorbent possessed good selectivity for phosphate even in the existence of competitive anions (such as Cl^-, $SO4^{2-}$, HCO^{3-}, NO^{3-}, F^- and $HCrO^{4-}$). The adsorption mechanisms are due to electrostatic attraction and the anion exchange of lanthanum ligand (Fig. 6b). More importantly, the dynamic test data were well consistent with the Thomas model in the continuous adsorption process, indicating the

feasibility for industrial practical applications. As a result, the cost-effective hydrogel adsorbent would have the potential for removing phosphate in wastewater treatment. A PDA-functionalized carboxyl methylcellulose and chitosan-based nanostructured adsorbent was found to efficiently remove Cd(II) (470.0 mg g^{-1}) and Cr(VI) (347.0 mg g^{-1}) (Li et al. 2020). PDA was also used as an intermediate layer to prepare chitosan/poly (L-lactic acid)-based porous nanofibrous membranes with high-performance for removal of Cu(II) (270.27 mg g^{-1}) (Zia et al. 2021). Recently, a kind of genipin-crosslinked PDA/chitosan/calcium alginate composite beads was developed for removing difenoconazole (66.5%) and nitenpyram (51.3%) (Zhou et al. 2022).

Polymer nanocomposites have attracted considerable attention in removing heavy metal ions because of the advantages from both nanomaterials and polymers. Wei and co-workers (Zeng et al. 2016) immobilize chitosan on the surface of multiwalled carbon nanotubes (MWCNTs) via combining dopamine chemistry and Michael addition reaction, leading to the MWCNT-based chitosan nanocomposites. The resulting nanocomposites showed apparently enhanced property for removing Cu(II) from aqueous solution when compared to the unmodified MWCNT. Taking into consideration of the multifunctionality of dopamine chemistry, this strategy for the preparation of nanocomposites should be a general approach for preparing highly efficient adsorbents in environmental applications. Magnetic nanocomposites also have been reported to have excellent removal capacity for heavy metal ions and organic pollutants. Liu et al. (Wang et al. 2016) prepared a magnetic nanocomposite via assembling PDA and chitosan onto the surface of Fe_3O_4 based on Schiff base reaction. Owing to the large surface area of nanoparticles and plentiful active groups of both PDA and chitosan, this nanocomposite was expected to have multiple interactions for the adsorption of pollutants. Batch tests indicated that this nano-biosorbent had highly efficient adsorption ability for the targeted metal ions and dyes. This nanocomposite had good adsorption capacities for Hg(II) (245.6 mg g^{-1}), Pb(II) (47 mg g^{-1}), Cr(VI) (151.6 mg g^{-1}), MB (204 mg g^{-1}) and malachite green (61 mg g^{-1}). In addition, it was found that this nano-biosorbent might be recovered and reused at least four times, and was able to keep good adsorption efficiency after each cycle. Therefore, the magnetic nanocomposites will be a potential adsorbing material for removing multiple pollutants.

Fly ash, produced during the combustion of coal for energy production, is an industrial by-product, which can serve as a low-cost adsorbent for metal ions (Ahmaruzzaman 2010). And, it has certain magnetism. Thus, it can act as a magnetic additive for the fabrication of adsorbents. Zhang et al. (Mu et al. 2020) reported that the heat treatment of fly ash at 750°C could generate C@magnetic fly ash, which was then functionalized with PDA, followed by mixture with chitosan to give a CS/polydopamine@C@magnetic fly ash (CPCMFA) adsorbent bead. The freeze-dried CPCMFA showed high adsorption capacity (57.02 mg/g) and excellent selectivity for Ag(I) in the copresence of Cu(II), Zn(II) and Ni(II) ions. More importantly, CPCMFA had high recyclability, and its adsorption capacity could be maintained up to 95.7% of the fresh adsorbent after five adsorption-desorption cycles.

Aerogels with some especial advantages (huge and tailored pore volumes, large specific surface area, as well as low density) have the potential ability to be used as adsorbents (Ren et al. 2018). A PDA-modified-chitosan (CS-PDA) aerogel was fabricated using glutaraldehyde to cross-link chitosan and simultaneously combined the self-polymerization of dopamine (Guo et al. 2018). The use of glutaraldehyde to cross-link chitosan could increase the adsorption stability and acid resistance, and PDA was able to improve the adsorption ability. The resulting CS-PDA aerogels showed remarkable adsorption capacity for removing metal ions and dyes, and had a maximum adsorption ability of 374.4 mg g^{-1} for Cr(VI) and 441.2 mg g^{-1} for Pb(II), respectively. Furthermore, the adsorption capacity of this aerogels could be still kept approximately 80% after eight adsorption-desorption cycles. As a result, the CS-PDA aerogels will be a promising alternative to the existing adsorbents for various pollutants because of the high adsorbing ability, economic rationality and superior recoverability.

The incorporation of specific inorganic materials into aerogels should be a useful approach to improve their adsorption capacity. Graphene oxide (GO) and its derivatives, as the latest members of the inorganic carbon-based materials, have aroused considerable interest in the adsorption removal of metal ions because of their good physicochemical performances, such as ultralarge surface area, high mechanical strength, ultralight weight and so on (Huang et al. 2019). A new PDA-functionalized GO/chitosan (GO@PDA/CS) composite aerogel was reported for U(VI) adsorption (Liao et al. 2018b). To obtain this composite aerogel, dopamine was employed to modify GO nanosheets to give the as-prepared GO@PDA nanosheets that could be cross-linked by chitosan to form 3D aerogel based on hydrogen bonding interaction between the plentiful hydroxyl and amino moieties in chitosan and the catechol and imine/amine moieties in GO@PDA. Compared with GO/chitosan aerogel, this resulting aerogel showed a more homogeneous and ordered 3D porous architecture and the increased active sites, which contributed to adsorption removal of U(VI). Based on the batch experiments, it was found that this aerogel had a quite rapid adsorption rate and accomplished its adsorption equilibrium within 15 min. The composite aerogel had the maximum adsorption capacity of 415.9 mg g^{-1} for U(VI). What's more, the composite aerogel showed well-pleasing thermal and mechanical stability and might keep its original adsorption efficiency after at least six cycle experiments. A PDA and chitosan cross-linked GO composite aerogel was reported to have a 3D porous network structure, which can be used for efficient Cr(VI) removal (maximum adsorption capacity: 312.05 mg g^{-1}) (Li et al. 2020). Recently, GO and MWCNTs were introduced into PDA-functionalized CS-based aerogel for highly selective recycle Gd(III) (150.86 mg g^{-1}) from end-of-life rare earth productions (Zhang et al. 2021).

Attapulgite (AT) is a plentiful, low-cost natural fibrous clay mineral that can be regarded as promising precursors for fabricating inorganic/organic aerogels. Owing to its good stability, high specific surface area, exchangeable cations and reactive –OH units on the surface, AT and its nanocomposites have showed broad potential application in the removal of U(VI) (Liu et al. 2018a). A 3D porous PDA-modified AT/chitosan aerogel with a loose and coarse surface could be obtained via a facile “sol-cryo” approach (Liao et al. 2018a). The resulting aerogel could rapidly adsorb U(VI) and the maximum adsorbing capacity reached up to 175.1 mg g^{-1}. After five adsorption-desorption cycles, it might keep 78%

adsorption efficiency. Therefore, this composite aerogel can be applied as a hopeful candidate for efficiently separating and recycling U(VI).

Membrane separation technique has been shown to become a prospective method to separate various emulsions and organic pollutants due to the excellent separation efficiency, low cost, as well as simple operability (Kim et al. 2018). Recently, a dually charged polyelectrolyte multilayer membrane was successfully fabricated by the layer-by-layer assembly of PDA and quaternized chitosan on polyethersulfone (PES) ultrafiltration membrane (Ouyang et al. 2019). This obtained multilayer membrane could be used for removing pharmaceuticals and personal care supplies. By controlling the number of layers (three bilayers), PDA (4 g L^{-1}) and NaCl (0.075 g L^{-1}) concentrations, the optimized membrane was ontained. This optimized membrane showed salt rejection capacity as K_2SO_4 > Na_2SO_4 > $MgSO_4$ > NaCl > KCl > $MgCl_2$ at neutral pH, and exhibited high rejection to atenolol (76.22%), carbamazepine (87.29%), as well as ibuprofen (89.85%). Besides, by tuning pH, the retention rates of atenolol and carbamazepine were raised to 81.67% and 92.50%, respectively, which indicated that this functionalized membrane surface possessed dually charged feature.

Alginate is also cost-effective biopolymers adsorbents for removing heavy metal ions and organic pollutants due to its abundant hydroxyl and carboxylate groups (Vu et al. 2017). Li's group (Li et al. 2016) showed a simple and efficient approach to prepare magnetic composites via modifying $CoFe_2O_4$ with PDA, followed by the mixture of the magnetic composites with sodium alginate (SA) and Ca^{2+} ions to give SA@CoFe2O4-PDA beads. The resulting beads showed remarkable adsorbing properties for MB, crystal violet, as well as malachite green. In addition, the materials had much higher maximum adsorbing capacities for both of MB (466.60 mg/g) and crystal violet (456.52 mg/g) than malachite green (248.78 mg/g). Compared to Na-electrolyte, Ca-electrolyte showed obvious negative influence on adsorbing MB and crystal violet but exhibited little influence on adsorbing malachite green. More importantly, the high saturation magnetization enabled the simple, convenient and fast separation and recovery of this adsorbent using an additional magnetic field.

A new class of hydrogel beads was prepared by incorporating PDA into alginate/poly(acrylamide) double network hydrogels, which showed efficient adsorption removal of MB (Zhang et al. 2018). It was thought that its high adsorption performance was on account of the cooperative effects between PDA and double network structure. The adsorption mechanism was assigned to the electrical interaction between MB and hydrogels. Furthermore, the desorption process of MB was able to be readily accomplished through rinsing in acidic water and ethanol solution, and its adsorption performance could be kept after five adsorption-desorption cycles.

Cr(VI), generated from industrial wastewater, is a kind of high poisonous metal ion that pollutes environment seriously (Xie et al. 2017). Zhai et al. (Yan et al. 2017) reported that new functionalized alginate hydrogel beads (HS-PDA@PEI-SA@PEI) were prepared synergistically using PDA-PEI-functionalized $CaCO_3$ composites, in which PEI could serve as a granule interior and surface modification agent and glutaraldehyde was used as a crosslinker. The resulting beads had hollow cavity architectures

and abundant reactive sites in its interior and surface, leading to the efficient removal of Cr(VI). The optimal hydrogel beads showed a superior adsorbing ability of 524.7 mg g^{-1}. In addition, recovery study indicated that the hydrogel beads had excellent regenerability, even after five cycles. In short, this strategy presented a remarkable bio-adsorbent due to the ultra-high Cr(VI) adsorption property, fast adsorbing rate, low cost, as well as easy recoverability. Recently the same group also combained the mussel and seaweed hydrogel-inspired methods to synthesize a ion-imprinted polymer using the PDA-PEI-functionalized $CaCO_3$ composites and SA as the functional platform for high-efficiency and selective adsorption of Pb(II) (357.4 mg g^{-1}) from wastewater (Shen et al. 2019).

The emerging forward osmosis technique has showed a potential application in wastewater treatment (Akther et al. 2015). Liu and co-workers (Liu et al. 2017) fabricated the layer-by-layer assembled forward osmosis membranes with multilayer polymer network to investigate their removal properties for heavy metal ions. The forward osmosis membranes were prepared through the assembly of multiple PEI and SA bilayers on the PDA-modified polyvinylidene fluoride supporting membranes. The resulting membranes had high rejection for Cu^{2+}, Ni^{2+}, Pb^{2+}, Zn^{2+} and Cd^{2+}. It was found that the three-layer membrane had more than 99.31% (in an active layer facing the feed solution mode) and 95.93% (in an active layer facing the draw solution mode) rejections for all the heavy metal ions, respectively. Experimental results also showed that the thickness of membranes, the hydrated radii of metal ions, and the heavy metal ion adsorption would have an effect on the high rejection.

A facile immobilization approach was used to load alginate, ferric oxide and dopamine onto fungal mycelium for fabricating a range of spherical composites that could be applied as underlying adsorbing materials for separating and removing thorium from water (Ding et al. 2019). As shown in Fig. 7, these adsorbents included magnetic γ-Fe_2O_3-functionalized fungal microspheres (FFMs), PDA-modified fungal microspheres (PFMs) and magnetic γ-Fe_2O_3 and PDA-coimmobilized fungal microspheres (FPFMs). By comparison, it was found that FPFMs showed the highest adsorbing capacity of 326.346 mg g^{-1} for thorium. In addition, FPFMs were able to be easily recovered and reused. The proposed mechanism for the adsorption process should be on account of the synergistic effects of chelation interaction, coordination and ion exchange on the heterogeneous surface of FPFMs.

Ouyang's group (Song et al. 2019) mixed Al-pillared montmorillonite (MT) with SA and $CaCl_2$ to generate microspheres that could be further modified with PDA and then were cross-linked by a combination of ethylenediamine and glutaraldehyde, resulting in the formation of core–shell/bead-like adsorbent materials. The resulting adsorbents could remove 94.85% As(V) at pH = 4 after 150 min, possess the maximum adsorption capacity of 61.94 mg/g, and keep more than 80% adsorption efficiency after six cycles.

3.2. Oil/water separation

At present, the challenge is to clean water resources that are being polluted by oils either in the production of routine shipping, run-offs from industry, dumping, or oil spills (Doshi et al. 2018). Oil spills have caused

great harm to both seas and land, and have a direct impact on the economy, ecology as well as human health (Ge et al. 2016). Therefore, there is a very urgent task to exploit efficient and recyclable separation materials for the treatment of oil-pollution problem. Although polysaccharide materials have shown particularly attractive prospects to solve this problem because of their low cost, non-toxicity and biodegradability, the natural hydrophilicity is a negative factor for their application in oil/water separation. The abundant catechol groups of PDA structure provide new thought to solve this problem. Here, PDA-functionalized polysaccharide materials for oil/water separation will be discussed as follows. Table 2 lists the application of oil/water separation using PDA-based polysaccharide materials.

Table 2
PDA-based polysaccharide materials for the oil/water separation.

Compositions	Separation efficiency	Ref.
Cellulose acetate, PDA, RGO, halloysite nanotubes	99.8%	(Liu et al. 2018b)
Cellulose acetate, PDA, RGO, g-C_3N_4	99.5%	(Li et al. 2017)
PDA, cotton	99.9%	(Mai et al. 2020)
Filter paper, PDA, SiO_2, hexadecyltrimethoxysilane	95.0%	(Tang et al. 2019)
Cellulose, PDA, $BaSO_4$	99.0%	(Yang et al. 2020)
PDA, cotton fabrics, octadecylamine	96%	(Yan et al. 2020)
PDA, cotton fabrics, AgNPs, CuNPs	99%	(Belal et al. 2020)
PDA, cotton fabrics, Ag/AgCl, polydimethylsiloxane	97.8%	(Liu et al. 2021)
BC, PDA, SiO_2	99.9%	(Wahid et al. 2021)
Cellulose acetate, PDA, sulfobetaine methacrylate	99.0%	(De Guzman et al. 2021)
Regenerated cellulose, PDA, attapulgite	99.0%	(Xie et al. 2021)
Chitin nanocrystals, PDA, GO	97.5%	(Ou et al. 2019)
Chitosan, PDA, RGO	98.8%	(Cao et al. 2017)
Chitosan, cotton fabrics, PDA,	99.0%	(Wang et al. 2020)
Chitosan, PDA, polyvinylidene fluoride	99.7%	(Zhang et al. 2019)

Cellulose-based aerogels have aroused considerable interest for application in oil/water separation (Xiao et al. 2018). Nevertheless, the inherent hydrophilicity of cellulose is almost always to the disadvantage of its use in oil/water separation (Mulyadi et al. 2016). The mussel-inspired surface chemistry opens a new door for cellulose surface modification so as to adjust its hydrophilicity. Inspired by dopamine chemistry,

Lu et al. (Gao et al. 2018) reported a facile and reproducible strategy to prepare superhydrophobic nanofibrillated cellulose (NFC)-based aerogels for oil/water separation. PDA coatings were used as the anchor to immobilize the NFC and octadecylamine (ODA), in which dopamine was coated on NFC surface based on its self-polymerization and ODA could be smoothly fixed to PDA coatings via Schiff-base reaction (Fig. 8). The resulting NFC-based aerogels had the low density of 6.04 mg/cm^3 and the large contact angle of 152.5°, leading to the superb buoyancy and the remarkable oil/water separation selectivity. It was observed that the NFC-based aerogels could fast absorb oil from oil-water mixture. Relying on the density and viscosity of the targeted liquids, the NFC-based aerogels had the maximum absorption capacity of 176 g/g. The new NFC-based aerogels with these excellent properties can be expected to serve as promising potential oil/water separation materials.

Membrane separation technique is a simple and efficient way for oil/water separation because of the low cost and easy operability (Gao et al. 2014). Liu's group (Liu et al. 2018b) prepared a kind of multifunctional PDA/RGO/HNTs/CA hybrid membranes that were composed of cellulose acetate (CA), reduced graphene oxide (RGO), halloysite nanotubes (HNTs) and PDA. The RGO/PDA/HNTs composites were first obtained through by the dopamine modification, and then were assembled on CA membrane surface through a vacuum filtration process, resulting in the formation the desired composite membrane. It was found that the membrane flux was able to be dramatically increased by the increase of HNTs ratio. The separating efficiencies of oil/water emulsion were around 99.85%, and the separation efficiencies of MB and CR, Cu^{2+}, and Cr^{3+} were 99.72%, 99.09%, 99.74% and 99.01%, respectively. What's more, the recycling and antifouling experiments demonstrated that this composite membrane still showed the outstanding anti-fouling performance after three cycles. In a similar work, Yu et al. (Li et al. 2017) used graphitic carbon nitride (g-C_3N_4) to replace HNTs to fabricate multifunctional PDA/RGO/g-C_3N_4/CA membrane that allowed to the fast, consecutive and synchronous flow separation of oil/water mixture and degradation of dyes. By increasing g-C_3N_4 content, the membrane flux could be enhanced gradually. The membranes had the separation rate of 99.5% for oil/water emulsion. In addition, the membranes were able to remove 99.8% MB and degrade it in oil-water mixture, thus realizing consecutive and synchronous flow oil/water separation and decomposition of MB in only one device. More significantly, this membrane might maintain stability after five cycles. These prominent properties should be assigned to the compact 2D-2D architecture of RGO and g-C_3N_4 with PDA surface modification, and RGO has the remarkable electron transport performance leading to effectively separate the photoelectron that is generated from g-C_3N_4 under light illumination. Overall, these composite membranes will have the potential for wastewater treatment.

A dual-superlyophobic membrane with selective oil-water separation performance was developed by one-step growth of PDA nanoparticles on biomass fibers surface, such as cotton and kapok (Fig. 9) (Mai et al. 2020). After being prewetted with water or oil, the dual-superlyophobic membranes were impermeable to the counterpart liquids, resulting in high oil–water separation efficiency of 99.98%. The resulting membranes also had superior properties for recovery and reuse. This convenient and eco-friendly strategy to fabricate dual-superlyophobic membranes is significant for practical separation applications. PDA also

could be used to functionalize paper fibers/cotton fabrics for forming superhydrophilic/underwater superoleophobic surface for oil/water separation (Belal et al. 2020; Liu et al. 2021; Tang et al. 2019; Yan et al. 2020; Yang et al. 2020).

A kind of superhydrophilic/underwater superoleophobic membrane was developed via mixing BC nanofibers with silica microparticles followed by the PDA modification (Wahid et al. 2021). The resulting composite membrane possessed high oil-water separation efficiency and flux rate (10,660 $Lm^{-2} h^{-1}$) with a small negative pressure (0.3–0.5 bar). This composite membrane also exhibited oil-in-water emulsion separation efficiency with high oil rejection (98.2%) and high flux rate (1250 $Lm^{-2} h^{-1}$) under the ultra-low pressure (< 0.1 bar). Furthermore, this composite membrane showed antifouling performance, recoverability, and stability under extreme conditions. These results indicated that this composite membrane is a promising candidate for oil-water and emulsion separation. Recently, the intramolecular Michael addition between dopamine and sulfobetaine methacrylate was applied to fabricate novel PDA-based nanoparticles that were then embedded into the cellulose acetate matrix, leading to a PDA-based mixed-matrix antifouling membrane with good oil-water separation ability (water flux: 583.64 $Lm^{-2} h^{-1}$ and separation efficiency: over 95%) (De Guzman et al. 2021).

For the past few years, Janus membranes with contrary wettability on both sides are capable of realizing on-demand oil-water separation via combining hydrophobic and hydrophilic properties (Zuo et al. 2020). Dai et al. (Xie et al. 2021) adopted regenerated cellulose membrane as a matrix, and then combined the bionic PDA surface modification and the superhydrophobic attapulgite spraying way to construct a new Janus membrane for oil-water separation. PDA could form a superhydrophilic surface on the membrane, while the superhydrophobic attapulgite was applied to produce a superhydrophobic surface by a spraying strategy. The novel Janus membrane possessed high separation efficiency (over 99%) towards all kinds of emulsions, and had acceptable renewability, remarkable environmental durability (acids, alkalis, and salts) and structural stability (10 cycles). This work opens a new chance to develop cost-effective Janus membranes for oil-water separation.

Chitin nanocrystals (ChNCs) generated from the removal of the amorphous domains of chitin, have aroused huge attention due to their characteristic acicular shape, high aspect ratio structures, large surface areas, as well as abundant surface function groups (Duan et al. 2018). To increase hydrophilicity of ChNCs, Liu and co-workers (Ou et al. 2019) modified ChNCs with PDA to give D-ChNCs. Subsequently, the resultant D-ChNCs were anchored onto stacked GO nanoplatelets, leading to the D-ChNCs/GO composite membranes. It was found that the needlelike D-ChNCs were distributed uniformly into interlayered GO nanoplatelets, and the hydrophilicity of this membrane was relied on the D-ChNCs content. The synergistic effects of the adjustable channel architecture of ChNCs and PDA surface functionalization would promote surface hydrophilicity, water permeability, as well as dyes and oil/water separation properties. This composite membrane presented high pure water flux (135.6 L $m^{-2} h^{-1}$) and excellent oleophobicity (the oil rejection ratio was more than 97.5%), and had the rejection ratios of 99.3% and 98.3% for MB and CR, respectively. In addition, the membrane possessed satisfying recoverability

and appropriate reproducibility. Therefore, these remarkable properties of the composite membranes endow it with especial ability for wastewater treatment.

Inspired by the inherent adhesion of dopamine, Cao et al. (Cao et al. 2017) exploited an eco-friendly way to fabricate RGO/PDA composite aerogel that could be strengthened via chitosan and modified via 1*H*,1*H*,2*H*,2*H*-perfluorodecanethiol (PFDT). PDA could be immobilized to RGO nanosheets through the self-polymerization of dopamine. The chitosan/RGO/PDA/ composite aerogel (CGA) was obtained with a 3D porous structure. Then, the fluorination of CGA using PFDT was to give perfluorinated CGA (*f*CGA). CGA exhibited super-amphiphilicity, but *f*CGA showed remarkable superhydrophobicity. It was found that both CGA and *f*CGA had high separation efficiency and high recoverable stability in oil-water separation (98.8%) and high organic adsorption ability. Based on the easy fabrication method and remarkable properties, these aerogels can be used as promising candidates for oil-spill accidents and oily wastewater treatment. PDA and chitosan might be applied to functionalize cotton fabric, resulting in formation of the superhydrophilic and underwater superoleophobic textiles (Wang et al. 2020). The modified cotton fabric showed excellent oil-water separation property with good separation efficiency (99%) and water flux (15,000 $Lm^{-2} h^{-1}$).

Recently, Yan's group (Zhang et al. 2019) developed a mussel-inspired one-step codeposition approach to fabricate a multifunctional underwater superoleophobic polyvinylidene fluoride/chitosan/dopamine (PVDF/CS&DA) membrane that was able to simultaneously accomplish high-efficiency oil-water separation and dyes removal (Fig. 10). With the help of biocatalyst of tyrosinase, PDA-based functionalization might be completed in a weak acid aqueous solution (pH 5.8–6.0) rather than traditional alkaline condition (pH 8.5), which offered a fascinating alternative approach toward mussel-inspired modification. This resulting membrane showed excellent underwater superoleophobicity and remarkable anti-oil-adhesiveness and self-cleaning abilities. The superwettability of this composite membrane enabled it to have an increased permeation flux (201.3 $Lm^{-2} h^{-1}$), a highly separated efficiency (99.7%) and remarkable anti-fouling performance in oil/water separation. Moreover, this composite membrane possessed remarkable adsorption capacities of 96.8% (MB) and 92.7% (orange G), and had a robust recyclability. As a consequence, this composite membrane incorporating high-efficiency oil/water separation and simultaneous dyes removal abilities has the huge potential in complicated wastewater treatment.

Jiang et al. (Zhao et al. 2015) deposited SA on the polyacrylonitrile (PAN) membrane with or without the help of PDA to give a series of SA/PAN, SA/PDA/PAN and SA/PEI–PDA/PAN membranes. By controlling the deposition conditions, the separation selectivity of the resulting membrane could be dramatically enhanced because the chemical components on the supported layer surface and the interface bonding strength could be synchronously tuned to realize the optimal free volume performance and swelling resistance. In the water/alcohol separation system, this SA/PEI–PDA/PAN membrane had separation factor up to 1807, which was significantly higher than other two membranes. The design and preparation of this SA/PEI–PDA/PAN membrane may provide an effective and simple strategy to develop high-selectivity membranes.

Covalent organic frameworks (COFs) have been found to be a novel kind of multipurpose porous organic polymers, and their attractive features, including easy modification, low density, high surface-to-volume ratio, well stability, as well as constant porosity, endow COFs with possible application prospect in separation science (Cao et al. 2019). Jiang's group (Yang et al. 2020) selected imine-type COFs as the fillers and dopamine-modified SA as the polymer matrix to prepare hybrid membranes. The dopamine modification could obviously increase the COF content up to 50 wt% in the hybrid membranes, and meanwhile the imine-linked COFs might improve the solubility selectivity for water and provide fast water transport pathways. The resulting hybrid membranes were used for the dehydration of ethanol/water mixed solution (water concentration of 10 wt%), showing high water concentration of around 98.7 wt% in permeate, and stable permeation flux of about 1500 g m^{-2} h^{-1}. As a consequence, the hybrid membranes had the desirable ethanol dehydration property and good operating stability. This work may provide an alternative strategy to prepare hybrid membranes with high separation selectivity through optimizing the polymer–filler interface.

3.3. Catalytic degradation of organic pollutants

Organic pollutants in wastewater have led to one of the most severe environmental problems today owing to their high toxicity and difficult degradability. Once organic pollutants emitted to the aquatic ecosystem will cause a variety of environmental problems, including blocking sewage treatment plants, disadvantageously influencing aquatic biota, as well as increasing biochemical oxygen. Hence, a green, efficient and economical method should be exploited to decrease organic pollutant concentrations before they are released into the ecological environment. Catalytic degradation of organic pollutants is one of the most fascinating strategies because of its high efficiency, simplicity, satisfactory recoverability, and facile operability. More importantly, this method can completely "eliminate" or "destroy" organic pollutants into degradable or low-toxic organic compounds (Ghanbari and Moradi 2017). The application of PDA-modified polysaccharide materials as catalysts for degrading organic pollutants will be described in the section below. Of course, pure polysaccharides cannot be directly used as catalysts for degradation of organic pollutants. During this process, PDA generally acts as an anchoring and reducing agent for the fabrication of metal (Ag or Au) nanoparticles. And, polysaccharides provide reaction platform for preparing or loading the metal nanoparticle catalysts through their large specific surface area and stable structures. In addition, inorganic materials (such as TiO_2, $Bi_{12}O_{17}Cl_2$, WO_3 and β-FeOOH) with photocatalytic activity also can be introduced into PDA-based polysaccharide systems to realize photocatalytic degradation of organic pollutants. Table 3 highlights the PDA-based polysaccharide materials to catalyze the degradation of organic pollutants.

Table 3
PDA-based polysaccharide materials to catalyze the degradation of organic pollutants.

Compositions	Descriptions	Ref.
CNCs, PDA, AgNPs, β-cyclodextrin	Catalytic reduction of 4-NP; activation energy: 33.88 kJ/mol; rate constant: 0.2554 min^{-1}; turnover frequency: 1077	(Tang et al. 2015)
Kapok fiber, PDA, AgNPs	Catalytic reduction of 4-NP; rate constant: 3.14×10^{-3} s^{-1}	(Cao et al. 2017)
Cellulose acetate, PDA, Ag–Fe_3O_4	Catalytic reduction of 4-NP; rate constant: 0.3504 min^{-1}	(Peng et al. 2018)
Cotton fabrics, PDA, 1-Dodecanethiol, β-FeOOH	Photocatalytic degradation of MB; MB was decomposed up to 90.0% after 180 min with visible light irradiation	(Cheng et al. 2020b)
Cotton fabrics, PDA, CuS nanoparticles	Photocatalytic degradation of MB; MB was decomposed up to 97.3% after 330 min with visible light irradiation	(Cheng et al. 2020a)
Cellulose acetate, PDA, RGO, $Bi_{12}O_{17}Cl_2$	Photocatalytic degradation of MB and p-chlorophenol; MB was decomposed up to 98.0% after 100 min with visible light irradiation; p-chlorophenol was decomposed up to 96.0% after 160 min with visible light irradiation	(Yu et al. 2017)
Cotton, PDA, Ag-WO_3	Photocatalytic degradation of C.I. Reactive Blue 19; C.I. Reactive Blue 19 was decomposed up to 98.0% after 180 min with visible light irradiation	(Fan et al. 2019)
Cellulose fibers, PDA, TiO_2	Photocatalytic degradation of MB; MB was decomposed up to 80.6% after 240 min with visible light irradiation	(Liu, et al. 2018)
BC, PDA, TiO_2	Photocatalytic degradation of MO, RhB and MB; MO was decomposed up to 95.1% after 30 min with visible light irradiation; RhB was decomposed up to 100% after 60 min with visible light irradiation; MB was decomposed up to 99.5% after 20 min with visible light irradiation	(Yang et al. 2020)
Chitin, PDA, AgNPs	Catalytic reduction of 4-NP, MB, RhB and MO	(Wang et al. 2017a)
Chitin nanocrystals, PDA, AgNPs	Catalytic reduction of 4-NP, MB, RhB and MO	(Wang et al. 2017b)
Chitosan, PDA, polystyrene, AgNPs	Catalytic degradation of pendimethalin; rate constant: 1.128 min^{-1}	(Xu et al. 2019)

Compositions	Descriptions	Ref.
Alginic acid, PDA, $Zn(OH)_2$ nanorods, AgNPs	Catalytic reduction of 4-NP and MB	(Lv et al. 2017)
Sodium alginate, PDA, N-doped porous carbon, CuNPs	Catalytic reduction of 4-NP; rate constant: 4.16×10^{-3} s^{-1}	(Zhao et al. 2021)

Nitrophenols are deemed to be one of the most refractory and toxic organic pollutants that are generated from agricultural and industrial waste-waters, their sources include companies that produce dyes, explosives and other products. Therefore, the reduction of toxic nitrophenols to benign aminophenols will solve an important environmental challenge. Metal nanoparticles have been become one of the most prospective catalysts for the reduction of nitrophenols due to their excellent catalytic activity, selectivity, durability, tenability and recoverability (Liu et al. 2019; Liu et al. 2021a). Tam et al. (Tang et al. 2015) reported a facile method to immobilize silver nanoparticles (AgNPs) to PDA-modified CNCs surface without additional stabilizer and reductant, in which AgNPs were formed *in-situ* via the reduction of Ag^+ due to the catecholamine oxidation (Fig. 11). The obtained CNC@PDA-AgNPs nanohybrids had the core-shell structures with abundant AgNPs decorating the CNCs surface, and could be applied in the catalytic degradation of 4-nitrophenol (4-NP) to 4-aminophenol (4-AP) by $NaBH_4$. It was found that the catalytic rate of CNC@PDA-AgNPs was six times higher than that of pristine AgNPs. Interestingly, this catalytic process was able to be promoted with the help of β-cyclodextrin because of the host-guest interaction between 4-NP and β-cyclodextrin. As a result, this composite nanocatalysts show a versatile platform for potential industrial applications. PDA was also applied to functionalize natural cellulose fiber via the surface modification to form hydrophilic surface, followed by the *in-situ* generation of AgNPs for catalyzing the 4-NP reduction (Cao et al. 2017).

Li and co-workers (Peng et al. 2018) decorated porous cellulose acetate (PCA) microspheres (generated from an emulsification process) with PDA to give PCA/PDA microspheres that were then used as support for $Ag–Fe_3O_4$ nanoparticles (SFNPs) through a one-pot in-situ strategy without the use of additional reductants. The obtained PCA/PDA/SFNPs showed remarkable catalytic activity in the 4-NP reduction. Furthermore, the reaction rate was significantly higher than SFNPs deposited on deacetylated porous cellulose acetate microspheres. The elevated catalytic property should be on account of the enhanced adsorption performance and dispersing property of SFNPs through introducing plentiful amine and catechol moieties of PDA into the PCA nanoporous architecture.

A superhydrophobic and lipophilic cotton fabric with was oil-water separation ability prepared through *in-situ* generating β-FeOOH nanorods on the PDA-functionalized cotton fabric, followed by a surface modification via 1-Dodecanethiol (Fig. 12a) (Cheng et al. 2020b). PDA coating could contribute to binding

Fe^{3+} by chelation. The oil-water separation efficiency of the resulting cotton fabric reached up to 98% and its recoverability exceeded 50 cycles. Interestingly, the functionalized cotton fabric could be employed as remarkable light-driven photocatalyst for the decomposition of MB (90.0%) and exhibited good stability and recoverability (5 cycles). The possible photocatalytic mechanism was shown in Fig. 12b. The photocatalytic mechanism was attributed to the $\cdot O_2^-$ and ·OH radicals to facilitate MB decomposition into CO_2 and H_2O, in which the β-FeOOH might be used as a semiconductive catalyst to produce electron (e^-) and hole pairs (h^+) to accelerate the formation of$\cdot O_2^-$ and ·OH radicals. This study opens a new door for exploiting multifunctional textiles with photocatalytic activity and particular wettability. The photocatalytic cotton fabrics also could be prepared via the deposition of CuS nanoparticles on cotton fabric surface with the help PDA, and might be applied for the photocatalytic degradation of MB (Cheng et al. 2020a).

$Bi_{12}O_{17}Cl_2$, a new type of nontoxic, chemically stable and layered materials, has attracted much research interest in the environment treatment field, especially in the visible light photocatalytic degradation of pollutants (Zhou et al. 2018). Yu et al. (Yu et al. 2017) used dopamine to modify GO and $Bi_{12}O_{17}Cl_2$ to generate RGO/PDA/$Bi_{12}O_{17}Cl_2$ composites that was then anchored to the commercial CA membrane via vacuum filtration approach. Dopamine might reduce GO and serve as a crosslinker, and RGO might effectively segregate the electron-hole pairs under visible light irradiation. The photocatalytic activities of the resulting membrane were estimated via the photodegradation of MB and 4-chlorophenol using visible light (> 400 nm) illumination. Photocatalytic experiments indicated that the obtained membranes showed 98% and 96% removal efficiency for MB and 4-chlorophenol, respectively. What's more, this membrane was able to concurrently accomplish dyes degradation and oil-water separation. This composite membrane also showed remarkable stability, and had obvious antifouling capacity and recyclability. In short, the photocatalytic composite membrane provides a fresh perspective for wastewater treatment. WO_3 also can be used as photocatalytic materials. The incorporation of photocatalytic WO_3 into PDA-coated regenerated cellulose films could form photocatalyst for the photocatalytic decomposition of C.I. Reactive Blue 19 (degradation efficiency: 98%) (Fan et al. 2019).

TiO_2 has been a popular inorganic material because of its good photocatalytic ability, excellent chemical stability in acidic and oxidative conditions, satisfactory photoelectric performances, nontoxicity and low cost (Zhao et al. 2019). Liu’s group (Qin et al. 2019) uniformly immobilized TiO_2 to the surface of cellulose fibre by the PDA coating, leading to a kind of photocatalytic paper. The photocatalytic ability of the resultant paper was determined in the degradation of MO using UV light irradiation. The results indicated that the introduction of PDA-functionalized cellulose fibre could improve the photocatalytic effect of this composite paper. And, this composite paper was rather stable in repeated tests. This work presents a novel strategy to fabricate photocatalytic paper with enhanced photocatalytic activity. A PDA-coated cellulose-based TiO_2 nanocomposite fibers was reported for photocatalytic degradation of MB (Fig. 13) (Liu et al. 2018). The nanocomposite fibers showed the elevated adsorption ability for removing Pb(II) (20 mg g^{-1}) and MB (15 mg g^{-1}). In addition, 80.6% of MB would be decomposed via the

nanocomposite fibers under UV radiation. The PDA-functionalized cellulose-based nanocomposite combined with the photocatalytic TiO_2 possessed several advantages, such as low-energy consumption, cost-effective feature and renewable sources.

TiO_2 nanoparticles were also immobilized into PDA-modified BC for the preparation of nanocomposite membrane with elevated adsorption and photodegradation of MO, MB and RB (Fig. 14) (Yang et al. 2020). TiO_2 nanoparticles was found to be evenly distributed within the nanocomposite membrane with the help of PDA, which would obviously increase the surface area and provide additional active groups for removing organic pollutants (MO, MB and RB). Compared to commercial P25, the resulting nanocomposite membrane showed significantly higher adsorption capacity for MO (6.4 times), MB (5.7 times) and RB (4.8 times). In addition, the nanocomposite membrane had high photodegradation efficiencies of 95.1% for MO, 100% for RB and 99.5% for MB, respectively. What's more, this as-prepared nanocomposite membrane merely decreased 5.5% photocatalytic efficiency after 5 cycles, indicating the good reusability and stability. This work gives a new insight to develop high-performance photocatalysts for degrading organic pollutants based on a simple, green, and low-cost strategy.

Chitin has inert chemical properties, which hinder its actual applications. In order to address this problem, the mussel-inspired chemistry and a dissolving-coagulating-freezing dry process was combined prepare mesoporous chitin aerogels (Fig. 15) (Wang et al. 2017a). Benefiting from the characteristic mesoporous and nanofibrous structures as well as the good reducibility of catecholamine, AgNPs were able to be generated in-situ and be anchored in this aerogel matrix. The resulting AgNPs hybrid aerogels showed remarkable catalytic ability and easy retrievability for degrading 4-NP, MO, RhB and MB. Overall, the dopamine chemistry presents a simple method to activate chitin and further build AgNPs–chitin composite aerogel with excellent catalytic ability, which is able to offer an eco-friendly strategy for the use of renewable chitin resource in wastewater treatment.

Li's group (Wang et al. 2017b) used PDA to functionalize ChNCs to form PDA(ChNCs) that was then employed to in situ reduce Ag^+ to give $PDA(ChNCs)_{Ag}$, followed by a vacuum filtration process to generate multifunctional ultrafiltration AgNPs hybrid membranes (Fig. 16). The obtained hybrid membranes had plentiful interconnected nanopores, adjustable thickness from 100 to 4000 nm, and high permeation flux of 13 400 L m^{-2} h^{-1} bar^{-1}. The catalytic property of hybrid membranes was first tested in the 4-NP reduction, demonstrating its excellent catalytic activity. The combination of high catalytic activity and high permeation flux enable the membranes to have the continuous flow catalysis for degrading 4-NP, MO, RhB and MB in minutes. Meanwhile, the membranes could keep its property after repeated filtration. In addition, the hybrid membranes were also able to recycle Au^{3+} from water because AgNPs might reduce Au^{3+} to large AuNPs due to its higher reactivity.

The porous PDA-coated magnetic Fe_3O_4 chitin microspheres were prepared via a sol–gel transition method and could be further used to fabricate AuNPs hybrid microspheres through the *in-situ* reduction of Au^{3+} (Wang et al. 2015). The resulting AuNPs hybrid microspheres possessed high activity in the 4-NP

reduction and might maintain its catalytic efficiency after 10 successive cycles, clearly indicating that this chitin microspheres might serve as an efficient capping agent for AuNPs and prevent their aggregation during the reaction process. Moreover, this magnetic catalyst could be recovered easily for many cycles after application of an additional magnetic field.

Misuse and overuse of pesticides has caused considerable negative impacts in the environment including the pollution of water, soil, as well as foodstuffs (Mew et al. 2017). How to degrade pesticides effectively and conveniently is an urgent problem to be solved. Bai's group (Xu et al. 2019) reported a kind of simple, efficient and recyclable thin-film catalyst PDA@Ag/PS/chitosan that was prepared through oil-water interfacial layer-by-layer self-assembly (Fig. 17). Chitosan acted as the crosslinker to immobilize PDA@Ag microspheres, which could improve the film stability due to the electrostatic interactions between electropositive chitosan and electronegative PDA, as well as the covalent bonds between amino moieties of chitosan and catechol moieties of PDA. To estimate its catalytic activity, the resulting films were used for the catalytic degradation of a nitroaromatic pesticide, namely pendimethalin, indicating excellent catalytic activity. Furthermore, it was also observed that the composite films were able to be readily isolated from the reaction solution only using a tweezers, and might be reused for at least seven times with no obvious loss of its catalytic property. Based on its remarkable catalytic efficiency and recyclability, the composite films possess underlying application prospect in wastewater treatment. Recently, it was reported that PDA-functionalized chitosan hydrogel was doped with hollow silica nanoparticles and loaded with permanganate, and was subsequently attached to titanium tablet surface to achieve synchronous coagulation and photodegradation of diclofenac sodium under UV irradiation (Sun et al. 2021). Mn(V) and ·OH radicals were found to be responsible for the photocatalytic degradation process. Furthermore, the as-prepared hydrogel could be reused at least 10 times for the photodegradation of diclofenac sodium with no need for rinse process.

The abundant carboxylic acid groups in alginate not only make it negatively charged, but also lead to electrostatic interactions with metal ions. Therefore, alginate was able to be applied to fabricate inorganic nanomaterials (Hong et al. 2017). Li et al. (Lv et al. 2017) selected alginate as the reactant and structure-oriented reagent to fabricate $Zn(OH)_2$ rods whose morphologies and sizes were able to be accurately regulated by alginate owing to the potent binding ability of alginate with metal ions. The obtained $Zn(OH)_2$ rods might be functionalized with PDA to give $Zn(OH)_2$/PDA hybrid, and the PDA surface coating further provided the possibility of reducing Ag^+ to AgNPs, resulting in the generation of $Zn(OH)_2$/PDA/Ag nanotubes. The resulting nanotubes had high catalytic activity for 4-NP reduction. Besides, the composite catalyst had the ability to be reused for more than six times with no obvious decrease of catalytic activity. More importantly, the efficient and fast reaction rate enabled the sustained flow catalysis. For example, the continuous flow catalytic degradation of MB could be achieved by depositing the $Zn(OH)_2$/PDA/Ag catalyst on filtering membranes. The filtering membranes were able to be reused for tens of times with no obvious loss of its catalytic property. The combination of low-cost starting materials, simple preparation process, convenient operation and exceptional performance makes the composite catalyst have tremendous potential in the degradation of organic pollutants.

By the pyrolysis of CuNPs loaded PDA-functionalized alginate-based hydrogel, a kind of sandwich-like porous beads was prepared for the catalytic degradation of 4-NP (Zhao et al. 2021). The as-prepared sandwich-like porous beads had high surface area (622 m^2 g^{-1}), and CuNPs with the size of 10–30 nm evenly distributed in the porous beads. The PDA functionalization could efficiently enhance the mechanical strength and avoid the loss of CuNPs in the catalytic process. The porous beads showed high reaction rate constant (4.16×10^{-3} s^{-1}) in the 4-NP reduction reaction, and could be reused for over 10 times with high conversion (97.3%). As a result, the sandwich-like porous beads have the potential for application in the industrial catalysis.

3.4. Solar-driven water purification

In the 21st century, water crisis has been a global problem. People are making a lot of effort to provide dependable access to clean and safe water. Along with the growing populations, the pollution of fresh water, as well as global warming, the requirement for safe water has continued to be aggrandized. It is of great significance to address the global water crisis for improving the living quality and promoting economic prosperity and social stability. To solve water crisis, the solution should be environmentally friendly and do not cause further pressure for the supply of safe water resources. It is crucially important to weigh the relationship of energy consumption and clean water generation. In this context, the solar-driven water purification technology utilizing sunlight has been considered as a hopeful and sustainable pathway (Zhang et al. 2019). Photothermal agents play an important part in the solar-driven water evaporation technology. Great efforts have been made to enhance energy conversion efficiency via the choice of materials and the design of devices. PDA has been proved to have good light-harvesting capability and photothermal transformation feature, which distinctly contributes to the development of the high-performance solar-driven water evaporators (Wu et al. 2021). Polysaccharides are abundant and renewable natural polymers with the advantages of cost-effective and eco-friendly characteristics, which makes them superior candidates for the design and development of solar-driven water evaporators (Xu et al. 2021). Therefore, the PDA-based polysaccharide materials will be beneficial to prepare high-performance and cost-effective solar-driven water evaporators via the combination of the advantages of both PDA and polysaccharides. In the following section, we will discuss the potential of PDA-based polysaccharide materials for solar-driven water purification. Table 4 summarizes the application of PDA-based polysaccharide materials for the solar-driven water purification.

Table 4
PDA-based polysaccharide materials for the solar-driven water purification.

Compositions	Descriptions	Ref.
Cellulose, PDA	Solar evaporation rate: 1.36 kg m^{-2} h^{-1}; solar conversion efficiency: 86.0%	(Zhou et al. 2021)
Bacterial nanocellulose, PDA	Solar evaporation rate: 3.47 kg m^{-2} h^{-1}; solar conversion efficiency: 78.0%	(Jiang et al. 2017)
Cellulose, PDA, $Ti_3C_2T_x$ MXene	Solar evaporation rate: 2.08 kg m^{-2} h^{-1}; solar conversion efficiency: 93.6%	(Chen et al. 2021b)
Sodium alginate, PDA, poly(N-isopropylacrylamide)	Solar evaporation rate: 7.18 kg m^{-2} h^{-1}	(Xu et al. 2021)
Sodium alginate, PDA	Solar evaporation rate: 2.56 kg m^{-2} h^{-1}; solar conversion efficiency: 86.0%	(Zong et al. 2018)

By the combination of the advantages of PDA (light-harvesting feature and photothermal conversion property) and cellulose (most abundant and cheapest renewable resource), Li et al. (Zhou et al. 2021) reported a low-cost PDA-functionalized cellulose-based aerogel with superhydrophilicity and underwater superoleophobicity for solar-driven water purification (Fig. 18). It was found that the as-prepared aerogel converted solar energy into heat effectively. After being lighted via sun illumination, the average surface temperature of the aerogel was increased by 18 ^{o}C relative to the original temperature of 22 ^{o}C in both seawater and oil-polluted seawaters. The solar evaporation rate of the aerogel could reach up to 1.36 kg m^{-1} h^{-1} and its solar energy utilization rate was 86%. Furthermore, the aerogel presented good antifouling ability during the long-term water evaporation because of the excellent hydrophilicity and underwater lipophobicity. Meanwhile, the aerogel also showed good adsorption capacity for organic dyes (11.5 mg g^{-1} for MB and 16.5 mg g^{-1} for RB). It is believed that the study offers new chance to develop biomimetic photothermal devices for high-efficiency solar-enabled water purification. A PDA-functionalized BNC bilayer evaporator was also exploited for high-efficiency solar steam generation via the high-density loading of PDA nanoparticles within the BNC hydrogel (Jiang et al. 2017). The obtained bilayer evaporator had the evaporation rate of 1.13 kg m^{-1} h^{-1} and the evaporation efficiency of 78% under one sun illumination. The biodegradable bilayer solar evaporator will become a rational solution for alleviating global water crisis.

Recently, a hierarchical solar evaporator was designed for effective solar-driven water purification via the combination of PDA and MXene ($Ti_3C_2T_x$) with highly hydrated cellulose network (Fig. 19) (Chen et al. 2021b). The hydrophilic moieties of the highly hydrated cellulose network were able to bond H_2O through H-binding to generate more activated H_2O, but PDA and MXene could immensely improve photothermal transformation efficiencies through a photothermal synergy. The as-prepared solar evaporator possessed an excellent evaporation rate of 2.08 kg m^{-2} h^{-1} and energy efficiencies of 93.5% in one sun illumination. It was also found that H_2O in the hierarchical solar evaporator had a lower vaporization enthalpy of 1915

J g^{-1} compared to the bulk H_2O (2440 J g^{-1}). Raman spectra and DFT analyses indicated that the low vaporization enthalpy was on account of the presence of a mass of weakly H-bonded intermediate H_2O. Furthermore, the hierarchical solar evaporator presented long-term salt tolerance (30 days) and remarkable decontamination ability. The work is expected to provide a facile and efficient pathway for developing high-efficiency biomass-based solar water evaporator.

Inspired by pufferfish behaviors, Priestley et al. (Xu et al. 2021) designed a solar absorber gel for solar-driven water purification. The solar absorber gel was made up of the photothermal PDA layer, the sodium alginate network, as well as the thermo-responsive poly(*N*-isopropylacrylamide) hydrogel. PDA had the broad-band solar absorption and good photothermal transformation efficiencies, and could be applied to endow hydrogels with photothermal ability. Poly(*N*-isopropylacrylamide) hydrogel would show hydrophilic/hydrophobic change at the lower critical solution temperature (LCST, around 33 ^{o}C), leading to the absorption and release of H_2O. This may be applied to imitate pufferfish behaviors, in which the pufferfish would be subjected to the uptake and release of H_2O under danger. The as-prepared solar absorber gel had the water collection rate of 7.18 kg m^{-2} h^{-1} under sunlight. Furthermore, the solar absorber gel also possessed high rejection rates of 97.1% for R6G, 87.7% for MO, and 84.0% for 4-NP, respectively. More importantly, the solar absorber gel was used to purify lake water (Carnegie Lake, Princeton, NJ, USA) under natural sunlight, resulting in the drinking water. As a consequence, the novel solar absorber gel provides a cost-effective strategy for application in sustainable clean water production.

To enhance solar-thermal effect, Li's group (Zong et al. 2018) made use of alginate (as the structure-directing reagent) to induce PDA into nanofibrils (diameter of 40 nm and aspect ratio of 120) (Fig. 20). The PDA nanofibrils were observed to have superior absorbance and higher photothermal transformation efficiencies of 86% compared to traditional PDA nanoparticles. The higher absorbance should be due to the comparatively higher structural order and excitonic coupling. The PDA nanofibrils were subsequently applied for effective solar collection and photothermal transformation to build photo-thermoelectric generator (solar-electricity transformation efficiencies of 5.6%) and solar-thermal evaporator (evaporation rates of 2.56 kg m^{-2} h^{-1}). The novel photothermal PDA nanofibrils with renewable, biocompatible, low-cost and easily available features have the huge potential for the design and development of solar-thermal evaporator for applications in solar-driven water purification and solar electric power.

4. Conclusion And Outlook

The examples discussed in this review have indicated that PDA-based polysaccharides materials can be developed into various cost-effective and high-performance products (including hydrogels, aerogels, membrane, beads and nanocomposites) for water treatment, including adsorption of heavy metals and organic pollutants, oil/water separation, catalytic degradation of organic pollutants, as well as solar-driven water purification. PDA-based polysaccharides materials have several obvious advantages: a) polysaccharides (cellulose, chitosan, chitin and alginate) are biodegradable, biocompatible, renewable and low-cost; b) PDA-based surface modification is a simple and convenient process; c) PDA has

plentiful functional moieties (including catechol, amine, and phenyl groups) for binding heavy metals and organic pollutants through electrostatic, coordinate, chelate, H-bonding, and π-π stacking interactions; d) PDA can regulate the interfacial stability, compatibility and hydrophilicity; e) PDA possesses good light-harvesting capability and photothermal transformation feature. Under this background, PDA-based polysaccharides materials have been developed and shown new perspectives for water treatment.

At present, despite great progress in making PDA-based polysaccharide materials for water treatment, their study is only at an early stage. The development of efficient methods for preparing PDA-based polysaccharide materials may give them some unique performances and attractive functionalities. To meet the growing expectations, we think that it is vital to realize key challenges, and meanwhile it is also necessary to seize the opportunities.

First, the surface of polysaccharides can be easily modified via PDA formation. The abundant functional groups (such as catechol, amine and aromatic groups) of PDA give polysaccharides some particular performances. For instance, PDA-functionalized polysaccharides show enhanced bonding ability towards heavy metals and organic pollutants based on electrostatic, coordination, chelation, H-bonding, or π-π stacking interactions. And PDA coating may tailor the surface wettability of polysaccharides, which contributes to improving its oil-water separation efficiency and capability. PDA also can serve as an anchoring and reducing agent for the in-situ reduction of metal ions (specially Au^{3+} and Ag^{+}) into metal nanoparticles, resulting in the catalytic degradation of organic pollutants. In addition, PDA-functionalized polysaccharides may combine with photoactive inorganic materials (such as TiO_2, $Bi_{12}O_{17}Cl_2$, WO_3 and β-FeOOH) to accomplish photocatalytic degradation of organic pollutants. More importantly, PDA-functionalized polysaccharides are applied to design and develop high-performance and cost-effective solar-driven water evaporators due to the good light-harvesting capability and photothermal transformation characteristic of PDA. Nevertheless, opportunities and challenges coexist. The biggest challenge is to understand and explore PDA structure and formation mechanism. In detail, it is incomplete and sometimes controversial for the PDA structures and formation routes. And, experimental variables may lead to the influence of PDA structure and formation mechanism. In order to illustrate the above issues, more experiments and theoretical analysis (such as fundamental computer simulations and comprehensively structural analysis) should be performed to obtain convictive proofs or complete details. Meanwhile, the interactions between PDA and polysaccharides are also ambiguous. During the PDA formation process, the quinone intermediates can be generated to covalently conjugate with polysaccharides (especially chitosan) through Shiff-base or Michael addition reactions. In addition, H-bonding and metal coordination of catechol groups also may make a contribution.

Second, large-scale preparation of PDA is difficult. At present, PDA functionalization technique is only used for laboratory research. It is a challenging work to precisely and repeatedly control the physicochemical performances of PDA coatings and is not easy to guarantee yield. Also, it is inevitable to generate secondary reactions during PDA formation process. Due to the strong adhesion ability, PDA have the tendency to aggregate, which gives a difficulty to prepare various composite materials. It is

worthy of further study for how to realize large-scale efficient production and practical application of PDA.

Third, natural polyphenols (structural and functional analogues of dopamine) including tannic acid, epicatechin gallate, catechin, pyrogallol, epigallocatechin, gallic acid also have reported for the surface functionalization in various promising applications (Guo et al. 2021). Especially, tannic acid containing many catechol and pyrogallol groups can provide active sites for surface modification of various substrates based on π-π stacking, H-bond, metal coordination, electrostatic and hydrophobic interactions (Sileika et al. 2013). What's more, tannic acid forms metal – phenolic networks (MPNs) via metal coordination interactions with many metal ions (including Mg^{2+}, Cu^{2+}, Ca^{2+}, Cd^{2+}, Al^{3+}, Cr^{3+}, V^{3+}, Fe^{3+} and Zr^{4+}), which has developed into a novel material-independent surface functionalization strategy (Guo et al. 2014). Therefore, it is very promising to combine MPNs and polysaccharides for the preparation of cost-effective adsorbents for water treatment.

Fourth, besides water treatment, PDA-based polysaccharide materials also have made great progress in the energy and biomedical fields. For example, PDA chemistry can introduce excellent self-adhesive performance into polysaccharide-based materials, which may be applied to prepare tissue adhesives for hemostasis and wound healing (Ling et al. 2021). PDA-based polysaccharide materials are used to prepare drug carriers with high drug load and controlled-release behaviors (Wang et al. 2021). PDA-based polysaccharide materials have a significant potential for photothermal therapy (Liu et al. 2021b). Also, PDA-based polysaccharide materials are able to serve as high-performance Lithium-ion batteries (Kim and Pol 2018) and supercapacitors (Chen et al. 2020). Indeed, PDA-based polysaccharide materials have exhibited broad application prospect across various fields.

In summary, PDA-based polysaccharide materials have exhibited a bright future for water treatment. However, it is still a very long way to go from the laboratory to the large-scale industrial production. If the above-mentioned challenges and opportunities are well faced, PDA-based polysaccharide materials will provide great prospect to develop low-cost, renewable and efficient materials for utilization in water treatment. We hope that this review will not only give researchers a comprehensive understanding of PDA-based polysaccharide materials, but also inspire them to further enlarge the scope of the applications in environmental protection, even in other fields.

Abbreviations

4-AP	4-aminophenol
4-NP	4-nitrophenol
AgNPs	Silver nanoparticles
AuNPs	Gold nanoparticles
AT	Attapulgite
BC	Bacterial cellulose
BNC	Bacterial nanocellulose
CA	Cellulose acetate
ChNCs	Chitin nanocrystals
CNCs	Cellulose nanocrystals
CNFs	Cellulose nanofibrils
COFs	Covalent organic frameworks
CR	Congo red
CV	Crystal violet
DFT	Density functional theory
g-C_3N_4	Graphitic carbon nitride
GO	Graphene oxide
HNTs	Halloysite nanotubes
LCST	Lower critical solution temperature
MB	Methylene blue
MO	Methyl orange
MOFs	Metal–organic frameworks
MPNs	Metal–phenolic networks
MT	Montmorillonite
MWCNTs	Multiwalled carbon nanotubes
ODA	Octadecylamine
PAN	Polyacrylonitrile
PDA	Polydopamine
PEI	Polyethylenimine

PES	Polyethersulfone
PFDT	1*H*,1*H*,2*H*,2*H*-perfluorodecanethiol
PIP	Piperazine
PVDF	Polyvinylidene fluoride
R6G	Rhodamine 6G
RCM	Regenerated cellulose membrane
RGO	Reduced graphene oxide
RhB	Rhodamine B
SA	Sodium alginate
ST	Safranine T
TMC	1,3,5-trimesoyl chloride

Declarations

Conflicts of interest

There are no conflicts to declare.

Acknowledgements

This work was financially supported by the National Natural Science Foundation of China (No. 52163020, No. 22165029).

References

1. Ahmaruzzaman M (2010) A review on the utilization of fly ash. Prog Energy Combust Sci 36:327–363
2. Akther N, Sodiq A, Giwa A, Daer S, Arafat HA, Hasan SW (2015) Recent advancements in forward osmosis desalination: A review. Chem Eng J 281:502–522
3. Alves NM, Mano JF (2008) Chitosan derivatives obtained by chemical modifications for biomedical and environmental applications. Int J Biol Macromol 43:401–414
4. Avcu E, Bastan FE, Abdullah HZ, Rehman MAU, Avcu YY, Boccaccini AR (2019) Electrophoretic deposition of chitosan-based composite coatings for biomedical applications: A review. Prog Mater Sci 103:69–108
5. Belal AS, Khalil MMA, Soliman M, Ebrahim S (2020) Novel superhydrophobic surface of cotton fabrics for removing oil or organic solvents from contaminated water. Cellulose 27:7703–7719

6. Cao EJ, Duan WZ, Wang F, Wang AQ, Zheng Y (2017) Natural cellulose fiber derived hollow-tubular-oriented polydopamine: In-situ formation of Ag nanoparticles for reduction of 4-nitrophenol. Carbohydr Polym 158:44–50
7. Cao N, Lyu Q, Li J, Wang Y, Yang B, Szunerits S, Boukherroub R (2017) Facile synthesis of fluorinated polydopamine/chitosan/reduced graphene oxide composite aerogel for efficient oil/water separation. Chem Eng J 326:17–28
8. Cao S, Li B, Zhu RM, Pang H (2019) Design and synthesis of covalent organic frameworks towards energy and environment fields. Chem Eng J 355:602–623
9. Caputo HE, Straub JE, Grinstaff MW (2019) Design, synthesis, and biomedical applications of synthetic sulphated polysaccharides. Chem Soc Rev 48:2338–2365
10. Ghanbari F, Moradi M (2017) Application of peroxymonosulfate and its activation methods for degradation of environmental organic pollutants. Rev Chem Eng J 310:41–62
11. Chaule S, Hwang J, Ha SJ, Kang J, Yoon JC, Jang JH (2021) Rational Design of a High Performance and Robust Solar Evaporator via 3D-Printing Technology. Adv Mater 33:2102649
12. Cheng DS, Liu YH, Zhang YL, Ran JH, Bi SG, Deng ZM, Cai GM, Tang XN, Zhou Y, Wang X (2020a) Polydopamine-assisted deposition of CuS nanoparticles on cotton fabrics for photocatalytic and photothermal conversion performance. Cellulose 27:8443–8455
13. Cheng DS, Zhang YL, Bai X, Liu YH, Deng ZM, Wu JH, Bi SGJH, Ran Cai GM, Wang X (2020b) Mussel-inspired fabrication of superhydrophobic cotton fabric for oil/water separation and visible light photocatalytic. Cellulose 27:5421–5433
14. Chen RW, Yang Y, Huang QB, Ling H, Li XS, Ren JL, Zhang K, Sun RC, Wang XH (2020) A multifunctional interface design on cellulose substrate enables high performance flexible all-solid-state supercapacitors. Energy Storage Mater 32:208–215
15. Chen WJ, Ma HZ, Xing BS (2020) Electrospinning of multifunctional cellulose acetate membrane and its adsorption properties for ionic dyes. Int J Biol Macromol 158:1342–1351
16. Chen YM, Zhang L, Yang Y, Pang B, Xu WH, Duan GG, Jiang SH, Zhang K (2021a) Recent Progress on Nanocellulose Aerogels: Preparation, Modification, Composite Fabrication, Applications. Adv Mater 33:2005569
17. Chen Y, Yang J, Zhu L, Jia XH, Wang SZ, Li Y, Song HJ (2021b) An integrated highly hydrated cellulose network with a synergistic photothermal effect for efficient solar-driven water evaporation and salt resistance. J Mater Chem A 9:15482–15492
18. Crini G, Lichtfouse E, Wilson LD, Morin-Crini N (2019) Conventional and non-conventional adsorbents for wastewater treatment. Environ Chem Lett 17:195–213
19. De Guzman MR, Andra CKA, Ang MBMY, Dizon GVC, Caparanga AR, Huang SH, Lee KR (2021) Increased performance and antifouling of mixed-matrix membranes of cellulose acetate with hydrophilic nanoparticles of polydopamine-sulfobetaine methacrylate for oil-water separation. J Membr Sci 620:118881

20. Della Vecchia NF, Avolio R, Alfe M, Errico ME, Napolitano A, d'Ischia M (2013) Building-Block Diversity in Polydopamine Underpins a Multifunctional Eumelanin-Type Platform Tunable Through a Quinone Control Point. Adv Funct Mater 23:1331–1340
21. Derami HG, Jiang QS, Ghim D, Cao SS, Chandar YJ, Morrissey JJ, Jun YS, Singamaneni S (2019) A Robust and Scalable Polydopamine/Bacterial Nanocellulose Hybrid Membrane for Efficient Wastewater Treatment. ACS Appl Nano Mater 2:1092–1101
22. Ding CF, Sun YL, Wang YH, Li JB, Lin YN, Sun WY, Luo CN (2017) Adsorbent for resorcinol removal based on cellulose functionalized with magnetic poly(dopamine). Int J Biol Macromol 99:578–585
23. Ding HL, Zhang XN, Yang H, Luo XG, Lin XY (2019) Highly efficient extraction of thorium from aqueous solution by fungal mycelium-based microspheres fabricated via immobilization. Chem Eng J 369:37–50
24. Dong LQ, Deng RJ, Xiao HY, Chen F, Zhou YF, Li JK, Chen S, Yan B (2019) Hierarchical polydopamine coated cellulose nanocrystal microstructures as efficient nanoadsorbents for removal of Cr(VI) ions. Cellulose 26:6401–6414
25. Dong YD, Zhang H, Zhong GJ, Yao G, Lai B (2021) Cellulose/carbon Composites and their Applications in Water Treatment - a Review. Chem Eng J 405:126980
26. Doshi B, Sillanpaa M, Kalliola S (2018) A review of bio-based materials for oil spill treatment. Water Res 135:262–277
27. Dwivedi AD, Sanandiya ND, Singh JP, Husnain SM, Chae KH, Hwang DS, Chang YS (2017) Tuning and Characterizing Nanocellulose Interface for Enhanced Removal of Dual-Sorbate (AsV and CrVI) from Water Matrices. ACS Sustain Chem Eng 5:518–528
28. Duan B, Huang Y, Lu A, Zhang LN (2018) Recent advances in chitin based materials constructed via physical methods. Prog Polym Sci 82:1–33
29. Du X, Li LX, Li JS, Yang CW, Frenkel N, Welle A, Heissler S, Nefedov A, Grunze M, Levkin PA (2014) UV-Triggered Dopamine Polymerization: Control of Polymerization, Surface Coating, and Photopatterning. Adv Mater 26:8029–8033
30. Du ZJ, Mao Y, Zhang PF, Hu J, Fu JJ, You QJ, Yin J (2021) TPGS-Galactose-Modified Polydopamine Co-delivery Nanoparticles of Nitric Oxide Donor and Doxorubicin for Targeted Chemo-Photothermal Therapy against Drug-Resistant Hepatocellular Carcinoma. ACS Appl Mater Interfaces 13:35518–35532
31. Fan J, Yu D, Wang W, Liu BJ (2019) The self-assembly and formation mechanism of regenerated cellulose films for photocatalytic degradation of CI Reactive Blue 19. Cellulose 26:3955–3972
32. Furtado LM, Ando RA, Petri DFS (2020) Polydopamine-coated cellulose acetate butyrate microbeads for caffeine removal. J Mater Sci 55:3243–3258
33. Gandini A, Lacerda TM, Carvalho AJF, Trovatti E (2016) Progress of Polymers from Renewable Resources: Furans, Vegetable Oils, and Polysaccharides. Chem Rev 116:1637–1669
34. Gao RN, Xiao SL, Gan WT, Liu Q, Amer H, Rosenau T, Li J, Lu Y (2018) Mussel Adhesive-Inspired Design of Superhydrophobic Nanofibrillated Cellulose Aerogels for Oil/Water Separation. ACS

Sustain Chem Eng 6:9047–9055

35. Gao XF, Xu LP, Xue ZX, Feng L, Peng JT, Wen YQ, Wang ST, Zhang XJ (2014) Dual-Scaled Porous Nitrocellulose Membranes with Underwater Superoleophobicity for Highly Efficient Oil/Water Separation. Adv Mater 26:1771–1775
36. Ge J, Zhao HY, Zhu HW, Huang J, Shi LA, Yu SH (2016) Advanced Sorbents for Oil-Spill Cleanup: Recent Advances and Future Perspectives. Adv Mater 28:10459–10490
37. Guo DM, An QD, Xiao ZY, Zhai SR, Yang DJ (2018) Efficient removal of Pb(II), Cr(VI) and organic dyes by polydopamine modified chitosan aerogels. Carbohydr Polym 202:306–314
38. Guo J, Ping Y, Ejima H, Alt K, Meissner M, Richardson JJ, Yan Y, Peter K, von Elverfeldt D, Hagemeyer CE, Caruso F (2014) Engineering multifunctional capsules through the assembly of metal–phenolic networks. Angew Chem Int Ed 53:5546–5551
39. Guo YX, Sun Q, Wu FG, Dai YL, Chen XY (2021) Polyphenol-Containing Nanoparticles: Synthesis, Properties, and Therapeutic Delivery. Adv Mater 33:2007356
40. Gusain R, Kumar N, Ray SS (2020) Recent advances in carbon nanomaterial-based adsorbents for water purification. Coord Chem Rev 405:213111
41. Huang D, Wu JZ, Wang L, Liu XM, Meng J, Tang XJ, Tang CX, Xu JM (2019) Novel insight into adsorption and co-adsorption of heavy metal ions and an organic pollutant by magnetic graphene nanomaterials in water. Chem Eng J 358:1399–1409
42. Hong HJ, Kim BG, Hong J, Ryu J, Ryu T, Kim H, Park IS (2017) Enhanced Sr adsorption performance of MnO2-alginate beads in seawater and evaluation of its mechanism. Chem Eng J 319:163–169
43. Hong S, Wang Y, Park SY, Lee H (2018) Progressive fuzzy cation-pi assembly of biological catecholamines. Sci Adv 4:eaat7457
44. Jiang QS, Derami HG, Ghim D, Cao SS, Jun YS, Singamaneni S (2017) Polydopamine-filled bacterial nanocellulose as a biodegradable interfacial photothermal evaporator for highly efficient solar steam generation. J Mater Chem A 5:18397–18402
45. Kim PJ, Pol VG (2018) High Performance Lithium Metal Batteries Enabled by Surface Tailoring of Polypropylene Separator with a Polydopamine/Graphene Layer. Adv Energy Mater 8:1802665
46. Kim S, Chu KH, Al-Hamadani YAJ, Park CM, Jang M, Kim DH, Yu M, Heo J, Yoon Y (2018) Removal of contaminants of emerging concern by membranes in water and wastewater: A review. Chem Eng J 335:896–914
47. Krasucka P, Pan B, Ok YS, Mohan D, Sarkar B, Oleszczuk P (2021) Engineered biochar - A sustainable solution for the removal of antibiotics from water. Chem Eng J 405:126926
48. Lau J, Gray S, Matsuura T, Emadzadeh D, Chen JP, Ismail AF (2015) A review on polyamide thin film nanocomposite (TFN) membranes: History, applications, challenges and approaches. Water Res 80:306–324
49. Laureano-Anzaldo CM, Gonzalez-Lopez ME, Perez-Fonseca AA, Cruz-Barba LE, Robledo-Ortiz JR (2021) Plasma-enhanced modification of polysaccharides for wastewater treatment: A review.

Carbohydr Polym 252:117195

50. Lee H, Dellatore SM, Miller WM, Messersmith PB (2007) Mussel-inspired surface chemistry for multifunctional coatings. Science 318:426–430
51. Lee HA, Park E, Lee H (2020) Polydopamine and Its Derivative Surface Chemistry in Material Science: A Focused Review for Studies at KAIST. Adv Mater 32:1907505
52. Liao Y, Wang M, Chen DJ (2018a) Production of three-dimensional porous polydopamine-functionalized attapulgite/chitosan aerogel for uranium(VI) adsorption. J Radioanal Nucl Chem 316:635–647
53. Liao Y, Wang M, Chen DJ (2018b) Preparation of Polydopamine-Modified Graphene Oxide/Chitosan Aerogel for Uranium(VI) Adsorption. Ind Eng Chem Res 57:8472–8483
54. Li F, Yu ZX, Shi H, Yang QB, Chen Q, Pan Y, Zeng GY, Yan L (2017) A Mussel-inspired method to fabricate reduced graphene oxide/g-C3N4 composites membranes for catalytic decomposition and oil-in-water emulsion separation. Chem Eng J 322:33–45
55. Li LL, Wei ZY, Liu XW, Yang YH, Deng CX, Yu ZM, Guo Z, Shi JH, Zhu CZ, Guo W, Sun ZJ (2020) Biomaterials cross-linked graphene oxide composite aerogel with a macro-nanoporous network structure for efficient Cr (VI) removal. Int J Biol Macromol 156:1337–1346
56. Ling ZX, Chen ZK, Deng J, Wang YF, Yuan B, Yang X, Lin H, Cao J, Zhu XD, Zhang XD (2021) A novel self-healing polydopamine-functionalized chitosan-arginine hydrogel with enhanced angiogenic and antibacterial activities for accelerating skin wound healing. Chem Eng J 420:130302
57. Li SS, Wang XL, An QD, Xiao ZY, Zhai SR, Cui L, Li ZC (2020) Upon designing carboxyl methylcellulose and chitosan-derived nanostructured sorbents for efficient removal of Cd(II) and Cr(VI) from water. Int J Biol Macromol 143:640–650
58. Liu CK, Lei XB, Wang L, Jia JZ, Liang XY, Zhao XZ, Zhu H (2017) Investigation on the removal performances of heavy metal ions with the layer-by-layer assembled forward osmosis membranes. Chem Eng J 327:60–70
59. Liu FF, Liu X, Astruc D, Gu HB (2019) Dendronized triazolyl-containing ferrocenyl polymers as stabilizers of gold nanoparticles for recyclable two-phase reduction of 4-nitrophenol. J Colloid Interface Sci 533:161–170
60. Liu FF, Liu X, Chen F, Fu Q (2021a) Tannic Acid: A green and efficient stabilizer of Au, Ag, Cu and Pd nanoparticles for the 4-Nitrophenol Reduction, Suzuki-Miyaura coupling reactions and click reactions in aqueous solution. J Colloid Interface Sci 604:281–291
61. Liu FF, Liu X, Chen F, Fu Q (2021b) Mussel-inspired chemistry: A promising strategy for natural polysaccharides in biomedical applications. Prog Polym Sci 123:101472
62. Liu HY, Yang L, Zhan YF, Lan JW, Shang JJ, Zhou M, Lin SJ (2021) A robust and antibacterial superhydrophobic cotton fabric with sunlight-driven self-cleaning performance for oil/water separation. Cellulose 28:1715–1729
63. Liu R, Dai L, Si CL (2018) Mussel-Inspired Cellulose-Based Nanocomposite Fibers for Adsorption and Photocatalytic Degradation. ACS Sustain Chem Eng 6:15756–15763

64. Liu X, Xu XT, Sun J, Alsaedi A, Hayat T, Li JX, Wang XK (2018a) Insight into the impact of interaction between attapulgite and graphene oxide on the adsorption of U(VI). Chem Eng J 343:217–224
65. Liu YC, Tu WW, Chen MY, Ma LL, Yang B, Liang QL, Chen YY (2018b) A mussel-induced method to fabricate reduced graphene oxide/halloysite nanotubes membranes for multifunctional applications in water purification and oil/water separation. Chem Eng J 336:263–277
66. Liu YL, Ai KL, Liu JH, Deng M, He YY, Lu LH (2013) Dopamine-Melanin Colloidal Nanospheres: An Efficient Near-Infrared Photothermal Therapeutic Agent for In Vivo Cancer Therapy. Adv Mater 25:1353–1359
67. Liu YL, Ai KL, Lu LH (2014) Polydopamine and Its Derivative Materials: Synthesis and Promising Applications in Energy, Environmental, and Biomedical Fields. Chem Rev 114:5057–5115
68. Li XL, Lu HJ, Zhang Y, He F, Jing LY, He XH (2016) Fabrication of magnetic alginate beads with uniform dispersion of CoFe2O4 by the polydopamine surface functionalization for organic pollutants removal. Appl Surf Sci 389:567–577
69. Lv LL, Wu XC, Li MJ, Zong L, Chen YJ, You J, Li CX (2017) Modulating Zn(OH)(2) Rods by Marine Alginate for Templates of Hybrid Tubes with Catalytic and Antimicrobial Properties. ACS Sustain Chem Eng 5:862–868
70. Mahfoudhi N, Boufi S (2017) Nanocellulose as a novel nanostructured adsorbent for environmental remediation: a review. Cellulose 24:1171–1197
71. Mai VC, Das P, Zhou JJ, Lim TT, Duan HW (2020) Mussel-Inspired Dual-Superlyophobic Biomass Membranes for Selective Oil/Water Separation. Adv Mater Interfaces 7:1901756
72. Messina MS, Messina KMM, Bhattacharya A, Montgomery HR, Maynard HD (2020) Preparation of biomolecule-polymer conjugates by grafting-from using ATRP, RAFT, or ROMP. Prog Polym Sci 100:101186
73. Mew EJ, Padmanathan P, Konradsen F, Eddleston M, Chang SS, Phillips MR, Gunnell D (2017) The global burden of fatal self-poisoning with pesticides 2006-15: Systematic review. J Affect Disord 219:93–104
74. Mohammed N, Lian H, Islam MS, Strong M, Shi ZQ, Berry RM, Yu HY, Tam KC (2021) Selective adsorption and separation of organic dyes using functionalized cellulose nanocrystals. Chem Eng J 417:129237
75. Mu CQ, Zhang L, Zhang XM, Zhong LL, Li Y (2020) Selective adsorption of Ag (I) from aqueous solutions using Chitosan/polydopamine@C@magnetic fly ash adsorbent beads. J Hazard Mater 381:120943
76. Mulyadi A, Zhang Z, Deng YL (2016) Fluorine-Free Oil Absorbents Made from Cellulose Nanofibril Aerogels. ACS Appl Mater Interfaces 8:2732–2740
77. Nasrollahzadeh M, Sajjadi M, Iravani S, Varma RS (2021) Starch, cellulose, pectin, gum, alginate, chitin and chitosan derived (nano) materials for sustainable water treatment: A review. Carbohydr Polym 251:116986

78. Nayak K, Kumar A, Das P, Tripathi BP (2021) Amphiphilic antifouling membranes by polydopamine mediated molecular grafting for water purification and oil/water separation. J Membr Sci 630:119306
79. Ou XF, Yang XH, Zheng JQ, Liu MX (2019) Free-Standing Graphene Oxide-Chitin Nanocrystal Composite Membrane for Dye Adsorption and Oil/Water Separation. ACS Sustain Chem Eng 7:13379–13390
80. Ouyang ZY, Huang ZH, Tang XY, Xiong CH, Tang MD, Lu YT (2019) A dually charged nanofiltration membrane by pH-responsive polydopamine for pharmaceuticals and personal care products removal. Sep Purif Technol 211:90–97
81. Pan XQ, Gu ZP, Chen WM, Li QB (2021) Preparation of biochar and biochar composites and their application in a Fenton-like process for wastewater decontamination: A review. Sci Total Environ 754:142104
82. Patil N, Jerome C, Detrembleur C (2018) Recent advances in the synthesis of catechol-derived (bio)polymers for applications in energy storage and environment. Prog Polym Sci 82:34–91
83. Peng S, Gao F, Zeng D, Peng C, Chen YM, Li M (2018) Synthesis of Ag-Fe3O4 nanoparticles supported on polydopamine-functionalized porous cellulose acetate microspheres: catalytic and antibacterial applications. Cellulose 25:4771–4782
84. Pillai CKS, Paul W, Sharma CP (2009) Chitin and chitosan polymers: Chemistry, solubility and fiber formation. Prog Polym Sci 34:641–678
85. Ponzio F, Barthes J, Bour J, Michel M, Bertani P, d'Ischia M, Ball V (2016) Oxidant Control of Polydopamine Surface Chemistry in Acids: A Mechanism-Based Entry to Superhydrophilic-Superoleophobic Coatings. Chem Mater 28:4697–4705
86. Qin ZZ, Liu WX, Chen HB, Chen J, Wang HL, Song ZP (2019) Preparing photocatalytic paper with improved catalytic activity by in situ loading poly-dopamine on cellulose fiber. Bull Mater Sci 42:54
87. Ren WJ, Gao JK, Lei C, Xie YB, Cai YR, Ni QQ, Yao JM (2018) Recyclable metal-organic framework/cellulose aerogels for activating peroxymonosulfate to degrade organic pollutants. Chem Eng J 349:766–774
88. Schwarzenbach RP, Egli T, Hofstetter TB, von Gunten U, Wehrli B (2010) Global Water Pollution and Human Health. Annu Rev Environ Resour 35:109–136
89. Shen W, Jiang X, An QD, Xiao ZY, Zhai SR, Cui L (2019) Combining mussel and seaweed hydrogel-inspired strategies to design novel ion-imprinted sorbents for ultra-efficient lead removal from water. New J Chem 43:5495–5502
90. Sileika TS, Barrett DG, Zhang R, Lau KHA, Messersmith PB (2013) Colorless Multifunctional Coatings Inspired by Polyphenols Found in Tea, Chocolate, and Wine. Angew Chem Int Ed 52:10766–10770
91. Song YC, Wang SY, Yang LY, Yu D, Wang YG, Ouyang XK (2019) Facile fabrication of core-shell/bead-like ethylenediamine-functionalized Al-pillared montmorillonite/calcium alginate for As (V) ion adsorption. Int J Biol Macromol 131:971–979

92. Sun DT, Peng L, Reeder WS, Moosavi SM, Tiana D, Britt DK, Oveisi E, Queen WL (2018) Rapid, Selective Heavy Metal Removal from Water by a Metal-Organic Framework/Polydopamine Composite. ACS Cent Sci 4:349–356
93. Sun Q, Zheng HL, Hu XB, Salam M, Sun ML, Zhao C, Bao B (2021) Titanium-based hollow silica nanocarrier doped hydrogel for ultraviolet assisted removal of diclofenac sodium. Sep Purif Technol 274:118694
94. Tang JT, Shi ZQ, Berry RM, Tam KC (2015) Mussel-Inspired Green Metallization of Silver Nanoparticles on Cellulose Nanocrystals and Their Enhanced Catalytic Reduction of 4-Nitrophenol in the Presence of beta-Cyclodextrin. Ind Eng Chem Res 54:3299–3308
95. Tang JT, Song Y, Zhao FP, Spinney S, Bernardes JD, Tam KC (2019) Compressible cellulose nanofibril (CNF) based aerogels produced via a bio-inspired strategy for heavy metal ion and dye removal. Carbohydr Polym 208:404–412
96. Tang XD, Wang XF, Tang C, Ma JP, Zhang SY, Li ZF, Dong FY (2019) PDA-assisted one-pot fabrication of bioinspired filter paper for oil-water separation. Cellulose 26:1355–1366
97. Tao BL, Lin CC, Yuan Z, He Y, Chen MW, Li K, Hu JW, Yang YL, Xia ZZL, Cai KY (2020) Near infrared light-triggered on-demand Cur release from Gel-PDA@Cur composite hydrogel for antibacterial wound healing. Chem Eng J 403:126182
98. Thompson KA, Shimabuku KK, Kearns JP, Knappe DRU, Summers RS, Cook SM (2016) Environmental Comparison of Biochar and Activated Carbon for Tertiary Wastewater Treatment. Environ Sci Technol 50:11253–11262
99. Vu HC, Dwivedi AD, Le TT, Seo SH, Kim EJ, Chang YS (2017) Magnetite graphene oxide encapsulated in alginate beads for enhanced adsorption of Cr(VI) and As(V) from aqueous solutions: Role of crosslinking metal cations in pH control. Chem Eng J 307:220–229
100. Wang B, Liu J, Niu DY, Wu NQ, Yun WT, Wang WD, Zhang KX, Li GF, Yan SF, Xu GH, Yin JB (2021) Mussel-Inspired Bisphosphonated Injectable Nanocomposite Hydrogels with Adhesive, Self-Healing, and Osteogenic Properties for Bone Regeneration. ACS Appl Mater Interfaces 13:32673–32689
101. Wang D, Yuan HM, Chen YT, Ni YH, Huang LL, Mondal AK, Lin S, Huang F, Zhang H (2020a) A cellulose-based nanofiltration membrane with a stable three-layer structure for the treatment of drinking water. Cellulose 27:8237–8253
102. Wang GH, Zhang JW, Lin SJ, Xiao HY, Yang Q, Chen S, Yan B, Gu YC (2020b) Environmentally friendly nanocomposites based on cellulose nanocrystals and polydopamine for rapid removal of organic dyes in aqueous solution. Cellulose 27:2085–2097
103. Wang M, Peng M, Zhu J, Li YD, Zeng JB (2020) Mussel-inspired chitosan modified superhydrophilic and underwater superoleophobic cotton fabric for efficient oil/water separation. Carbohydr Polym 244:116449
104. Wang Q, Astruc D (2020) State of the Art and Prospects in Metal-Organic Framework (MOF)-Based and MOF-Derived Nanocatalysis. Chem Rev 120:1438–1511

105. Wang YT, Li Y, Liu SL, Li B (2015) Fabrication of chitin microspheres and their multipurpose application as catalyst support and adsorbent. Carbohydr Polym 120:53–59
106. Wang YW, Kong QS, Ding BB, Chen YJ, Yan XF, Wang SW, Chen FS, You J, Li CX (2017a) Bioinspired catecholic activation of marine chitin for immobilization of Ag nanoparticles as recyclable pollutant nanocatalysts. J Colloid Interface Sci 505:220–229
107. Wang YW, Zhu LT, You J, Chen FS, Zong L, Yan XF, Li CX (2017b) Catecholic Coating and Silver Hybridization of Chitin Nanocrystals for Ultrafiltration Membrane with Continuous Flow Catalysis and Gold Recovery. ACS Sustain Chem Eng 5:10673–10681
108. Wang Y, Zhang Y, Hou C, Liu MZ (2016) Mussel-inspired synthesis of magnetic polydopamine-chitosan nanoparticles as biosorbent for dyes and metals removal. J Taiwan Inst Chem E 61:292–298
109. Wang ZX, Yang HC, He F, Peng SQ, Li YX, Shao L, Darling SB (2019) Mussel-Inspired Surface Engineering for Water-Remediation Materials. Matter 1:115–155
110. Wahid F, Zhao XJ, Duan YX, Zhao XQ, Jia SR, Zhong C (2021) Designing of bacterial cellulose-based superhydrophilic/underwater superoleophobic membrane for oil/water separation. Carbohydr Polym 257:117611
111. Wei X, Huang T, Nie J, Yang JH, Qi XD, Zhou ZW, Wang Y (2018) Bio-inspired functionalization of microcrystalline cellulose aerogel with high adsorption performance toward dyes. Carbohydr Polym 198:546–555
112. Wu XH, Cao SS, Ghim D, Jiang QS, Singamaneni S, Jun YS (2021) A thermally engineered polydopamine and bacterial nanocellulose bilayer membrane for photothermal membrane distillation with bactericidal capability. Nano Energy 79:105353
113. Xiao JL, Lv WY, Song YH, Zheng Q (2018) Graphene/nanofiber aerogels: Performance regulation towards multiple applications in dye adsorption and oil/water separation. Chem Eng J 338:202–210
114. Xie AT, Cui JY, Liu Y, Xue CG, Wang Y, Dai JD (2021) Preparation of Janus membrane based on biomimetic polydopamine interface regulation and superhydrophobic attapulgite spraying for on-demand oil-water emulsion separation. J Membr Sci 627:119242
115. Xie BH, Shan C, Xu Z, Li XC, Zhang XL, Chen JJ, Pan BC (2017) One-step removal of Cr(VI) at alkaline pH by UV/sulfite process: Reduction to Cr(III) and in situ Cr(III) precipitation. Chem Eng J 308:791–797
116. Xie CM, Wang X, He H, Ding YH, Lu X (2020) Mussel-Inspired Hydrogels for Self-Adhesive Bioelectronics. Adv Funct Mater 30:1909954
117. Xu T, Xu YX, Wang JY, Lu HJ, Liu WP, Wang J (2021) Sustainable self-cleaning evaporator for long-term solar desalination using gradient structure tailored hydrogel. Chem Eng J 45:128893
118. Xu XH, Ozden S, Bizmark N, Arnold CB, Datta SS, Priestley RD (2021) A Bioinspired Elastic Hydrogel for Solar-Driven Water Purification. Adv Mater 33:2007833
119. Xu XH, Sun L, Bai B, Wang HL, Suo YR (2019) Interfacial assembly of mussel-inspired polydopamine@Ag core-shell nanoparticles as highly recyclable catalyst for nitroaromatic pesticides

degradation. Sci Total Environ 665:133–141

120. Yang H, Wu H, Pan FS, Wang MD, Jiang ZY, Cheng QF, Huang C (2020) Water-selective hybrid membranes with improved interfacial compatibility from mussel-inspired dopamine-modified alginate and covalent organic frameworks. Chin J Chem Eng 28:90–97
121. Yang J, Xie AT, Cui JY, Chen YY, Lang JH, Li CX, Yan YS, Dai JD (2020) An acid-alkali-salt resistant cellulose membrane by rapidly depositing polydopamine and assembling BaSO4 nanosheets for oil/water separation. Cellulose 27:5169–5178
122. Yang L, Guo XT, Jin ZK, Guo WC, Duan GG, Liu XH, Li YW (2021) Emergence of melanin-inspired supercapacitors. Nano Today 37:101075
123. Yang LY, Chen CT, Hu Y, Wei F, Cui J, Zhao YX, Xu XR, Chen X, Sun DP (2020) Three-dimensional bacterial cellulose/polydopamine/TiO2 nanocomposite membrane with enhanced adsorption and photocatalytic degradation for dyes under ultraviolet-visible irradiation. J Colloid Interface Sci 562:21–28
124. Yang P, Zhu F, Zhang ZB, Cheng YY, Wang Z, Li YW (2021) Stimuli-responsive polydopamine-based smart materials. Chem Soc Rev 50:8319–8343
125. Yan XJ, Zhu XW, Ruan YT, Xing TL, Chen GQ, Zhou CX (2020) Biomimetic, dopamine-modified superhydrophobic cotton fabric for oil-water separation. Cellulose 27:7873–7885
126. Yan YZ, An QD, Xiao ZY, Zhai SR, Zhai B, Shi Z (2017) Interior multi-cavity/surface engineering of alginate hydrogels with polyethylenimine for highly efficient chromium removal in batch and continuous aqueous systems. J Mater Chem A 5:17073–17087
127. Yu ZX, Min X, Li F, Yin D, Peng YX, Zeng GY (2019) A mussel-inspired method to fabricate a novel reduced graphene oxide/Bi12O17Cl2 composites membrane for catalytic degradation and oil/water separation. Polym Adv Technol 30:101–109
128. Zeng GJ, Liu XH, Liu MY, Huang Q, Xu DH, Wan Q, Huang HY, Deng FJ, Zhang XY, Wei Y (2016) Facile preparation of carbon nanotubes based carboxymethyl chitosan nanocomposites through combination of mussel inspired chemistry and Michael addition reaction: Characterization and improved Cu2 + removal capability. J Taiwan Inst Chem E 68:446–454
129. Zia Q, Tabassum M, Meng JM, Xin ZY, Gong H, Li JS (2021) Polydopamine-assisted grafting of chitosan on porous poly (L-lactic acid) electrospun membranes for adsorption of heavy metal ions. Int J Biol Macromol 167:1479–1490
130. Zhai R, Chen XX, Jin MJ, Hu JG (2019) Synthesis of a polydopamaine nanoparticle/bacterial cellulose composite for use as a biocompatible matrix for laccase immobilization. Cellulose 26:8337–8349
131. Zhang C, Liang HQ, Xu ZK, Wang ZK (2019) Harnessing Solar-Driven Photothermal Effect toward the Water-Energy Nexus. Adv Sci 6:1900883
132. Zhang C, Wu BH, Zhou YS, Zhou F, Liu WM, Wang ZK (2020a) Mussel-inspired hydrogels: from design principles to promising applications. Chem Soc Rev 49:3605–3637

133. Zhang GF, Li YZ, Gao AL, Zhang QH, Cui J, Zhao S, Zhan XL, Yan YH (2019) Bio-inspired underwater superoleophobic PVDF membranes for highly-efficient simultaneous removal of insoluble emulsified oils and soluble anionic dyes. Chem Eng J 369:576–587
134. Zhang PB, Tang AQ, Wang ZH, Lu JY, Zhu BK, Zhu LP (2018) Tough poly(L-DOPA)-containing Double Network Hydrogel Beads with High Capacity of Dye Adsorption. Chin J Polym Sci 36:1251–1261
135. Zhang TM, Zhang WW, Xi H, Li QQ, Shen MX, Ying GB, Zhang JF (2021) Polydopamine functionalized cellulose-MXene composite aerogel with superior adsorption of methylene blue. Cellulose 28:4281–4293
136. Zhang W, Wang RX, Sun ZM, Zhu XW, Zhao Q, Zhang TF, Cholewinski A, Yang F, Zhao BX, Pinnaratip R, Forooshani PK, Lee BP (2020b) Catechol-functionalized hydrogels: biomimetic design, adhesion mechanism, and biomedical applications. Chem Soc Rev 49:433–464
137. Zhang YZ, Bian TT, Jiang R, Zhang Y, Zheng XD, Li ZY (2021) Bionic chitosan-carbon imprinted aerogel for high selective recovery of Gd(III) from end-of-life rare earth productions. J Hazard Mater 407:124347
138. Zhang YZ, Wang Y, Jiang Q, El-Demellawi JK, Kim H, Alshareef HN (2020) MXene Printing and Patterned Coating for Device Applications. Adv Mater 32:1908486
139. Zhao J, Fang CH, Zhu YW, He GW, Pan FS, Jiang ZY, Zhang P, Cao XZ, Wang BY (2015) Manipulating the interfacial interactions of composite membranes via a mussel-inspired approach for enhanced separation selectivity. J Mater Chem A 3:19980–19988
140. Zhao YX, Zhao YF, Shi R, Wang B, Waterhouse GIN, Wu LZ, Tung CH, Zhang TR (2019) Tuning Oxygen Vacancies in Ultrathin TiO2 Nanosheets to Boost Photocatalytic Nitrogen Fixation up to 700 nm. Adv Mater 31:1806482
141. Zhao ZY, Xiao ZY, Qin CR, Lv H, Qin LF, Niu WS, Zhai SR, An QD (2021) Sandwich-like N-C/Cu/N-C porous beads derived from alginate with enhanced catalytic activity and excellent recyclability for 4-nitrophenol reduction. Ind Crops Prod 164:113413
142. Zhou CY, Lai C, Xu P, Zeng GM, Huang DL, Li ZH, Zhang C, Cheng M, Hu L, Wan J, Chen F, Xiong WP, Deng R (2018) Rational Design of Carbon-Doped Carbon Nitride/Bi12O17Cl2 Composites: A Promising Candidate Photocatalyst for Boosting Visible-Light-Driven Photocatalytic Degradation of Tetracycline. ACS Sustain Chem Eng 6:6941–6949
143. Zhou JJ, Duan B, Fang Z, Song JB, Wang CX, Messersmith PB, Duan HW (2014) Interfacial Assembly of Mussel-Inspired Au@Ag@ Polydopamine Core-Shell Nanoparticles for Recyclable Nanocatalysts. Adv Mater 26:701–705
144. Zhou Q, Chen JJ, Jin B, Chu SJ, Peng RF (2021) Modification of ZIF-8 on bacterial cellulose for an efficient selective capture of U(VI). Cellulose 28:5241–5256
145. Zhou QZ, Wang WZ, Liu FM, Chen R (2022) Removal of difenoconazole and nitenpyram by composite calcium alginate beads during apple juice clarification. Chemosphere 286:131813
146. Zhao YM, Guo L, Shen W, An QD, Xiao ZY, Wang HS, Cai WJ, Zhai SR, Li ZC (2020) Function integrated chitosan-based beads with throughout sorption sites and inherent diffusion network for

efficient phosphate removal. Carbohydr Polym 230:115639

147. Zong L, Li MJ, Li CX (2018) Intensifying solar-thermal harvest of low-dimension biologic nanostructures for electric power and solar desalination. Nano Energy 50:308–315

148. Zou Y, Zhao JY, Zhu JY, Guo XY, Chen P, Duan GG, Liu XH, Li YW (2021) A Mussel-Inspired Polydopamine-Filled Cellulose Aerogel for Solar-Enabled Water Remediation. ACS Appl Mater Interfaces 13:7617–7624

149. Zuo J, Gu Y, Wei C, Yan X, Chen Y, Lang W (2020) Janus polyvinylidene fluoride membranes fabricated with thermally induced phase separation and spray-coating technique for the separations of both W/O and O/W emulsions. J Membr Sci 595:117475

Figures

Figure 1

PDA-based polysaccharide materials for water treatment

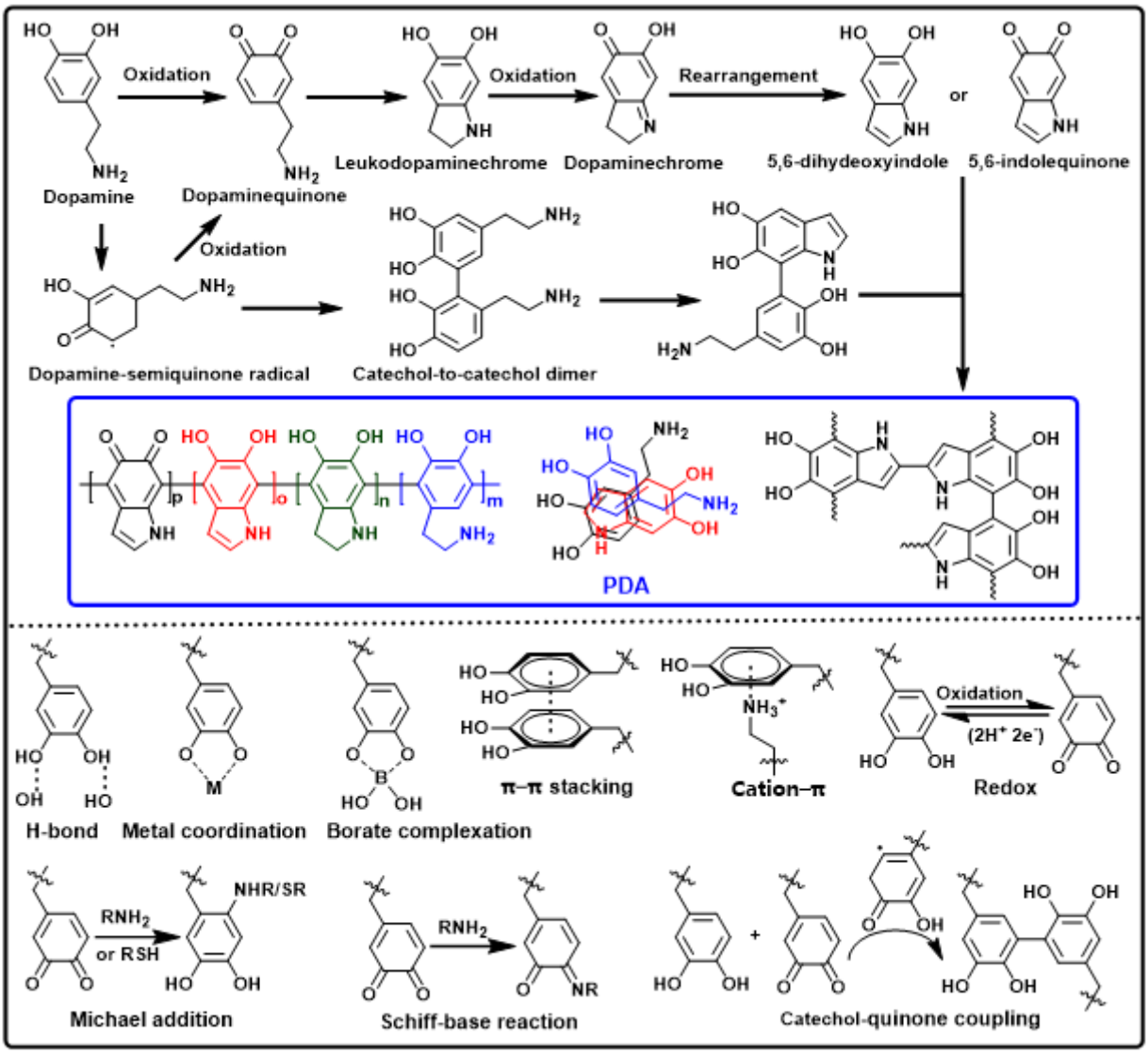

Figure 2

The proposed mechanisms for PDA formation and the representative interactions in dopamine chemistry.

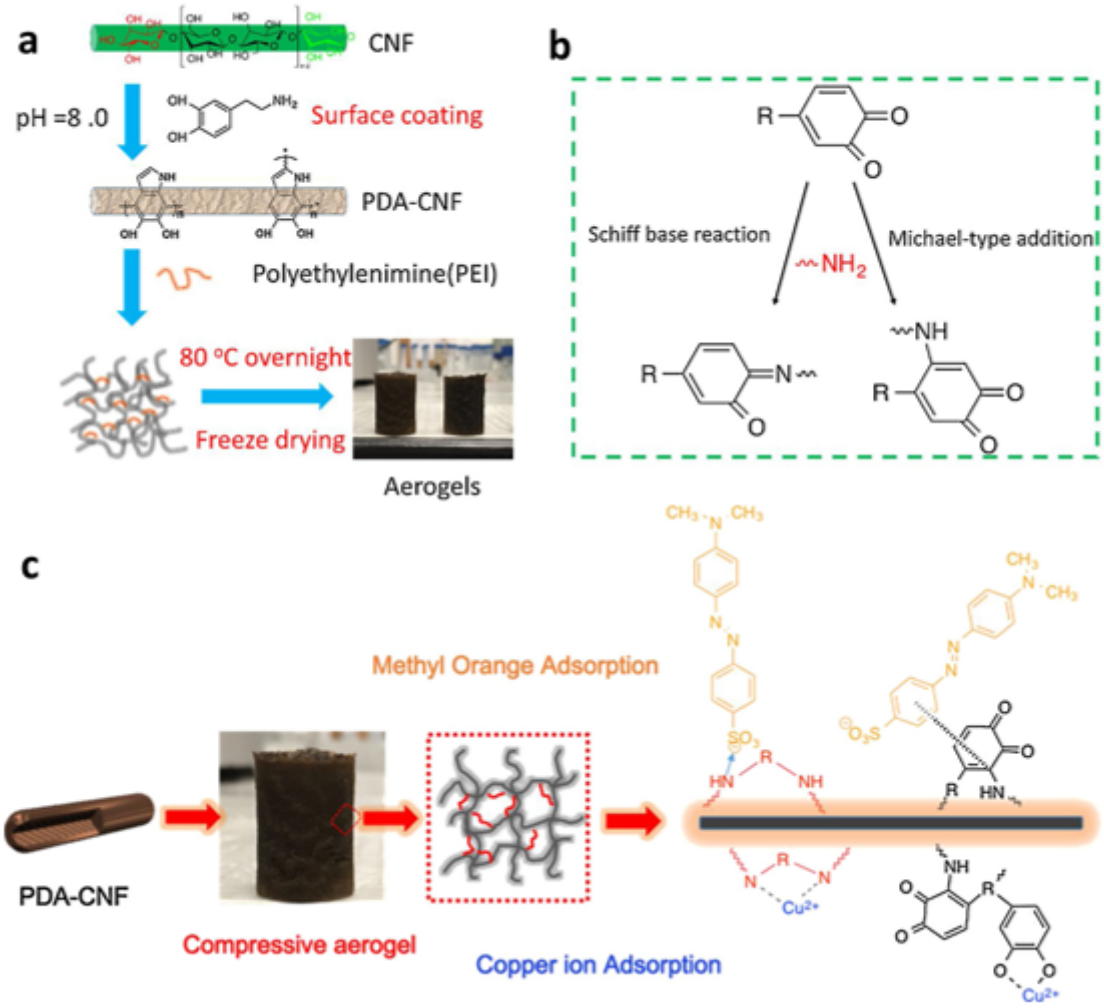

Figure 3

(a) Synthetic route of aerogels, (b) Possible crosslinking mechanism, (c) The interactions for adsorption process (Tang et al. 2019). Copyright 2019. Reproduced with permission from Elsevier.

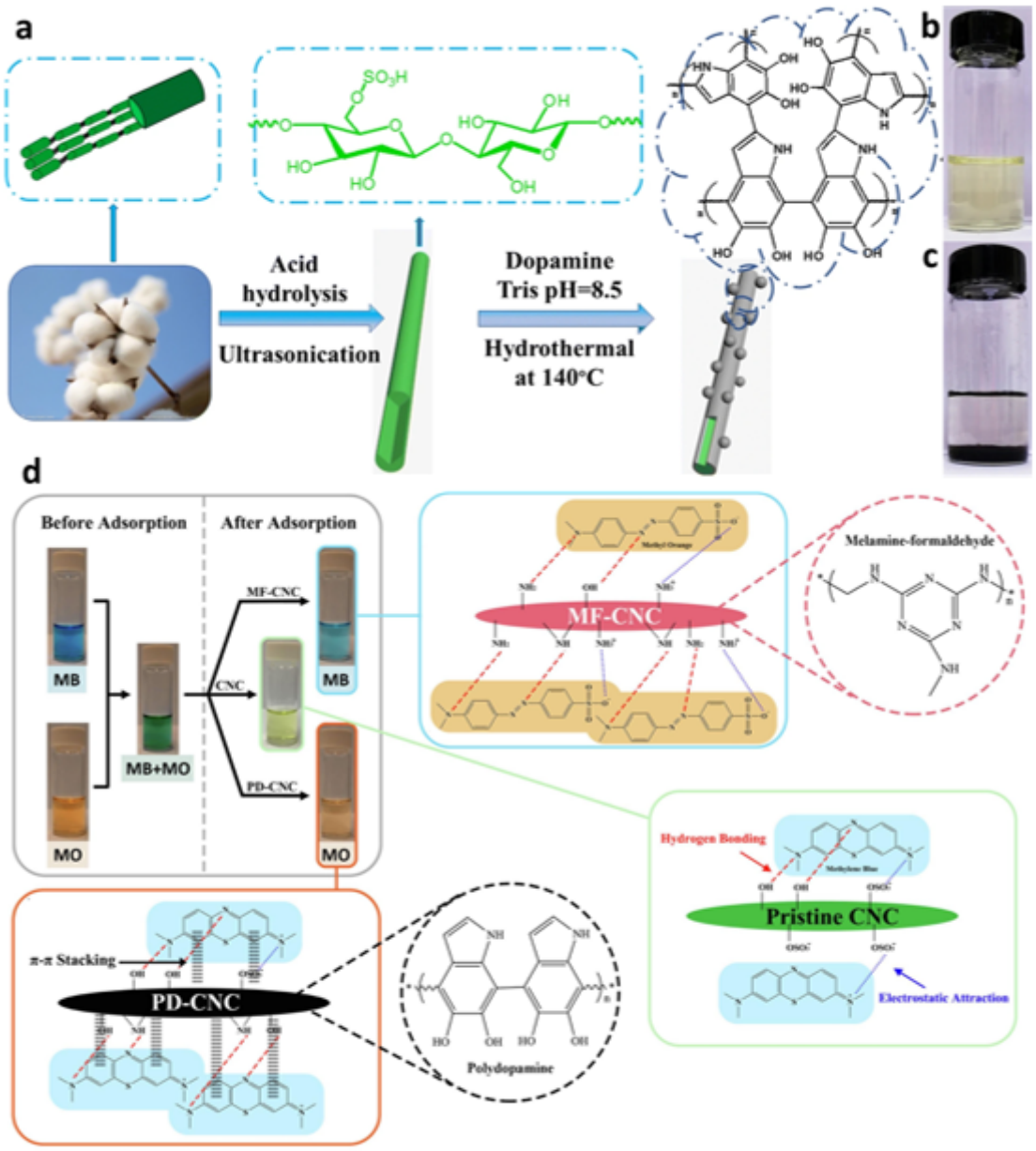

Figure 4

(a) Preparation of PDA-cellulose nanoadsorbents. (b,c) photographs of the Cr(VI) effluent and the mixture of PDA-cellulose nanoadsorbents and the effluent (Dong et al. 2019). Copyright 2019. Reproduced with permission from Springer Nature. (d) Schematic diagram of selective adsorption of dyes via PDA-functionalized CNCs (Mohammed et al. 2021). Copyright 2021. Reproduced with permission from Elsevier.

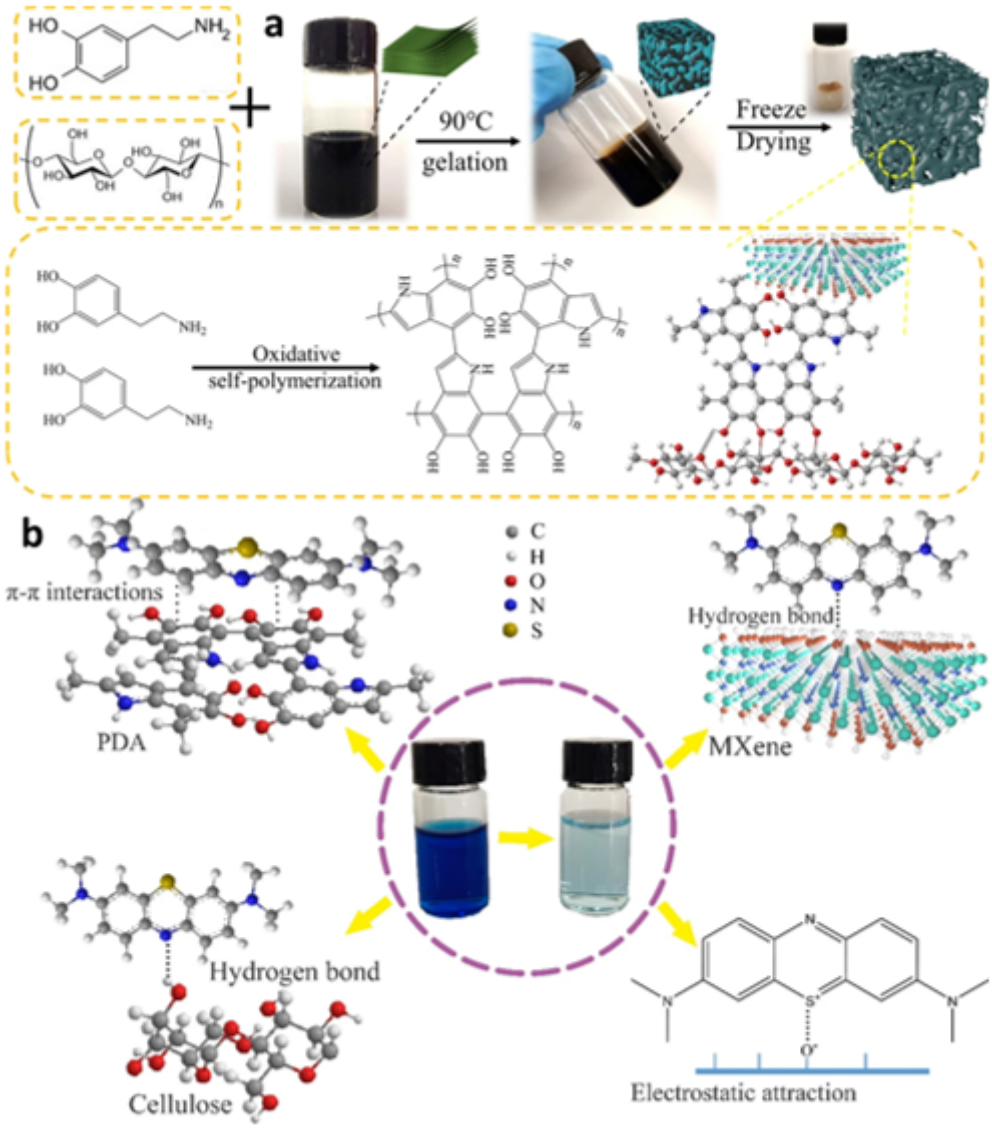

Figure 5

Preparation of PDA-functionalized cellulose-MXene composite aerogels (a) and the proposed adsorption mechanisms (b) (Zhang et al. 2021). Copyright 2021. Reproduced with permission from Springer Nature.

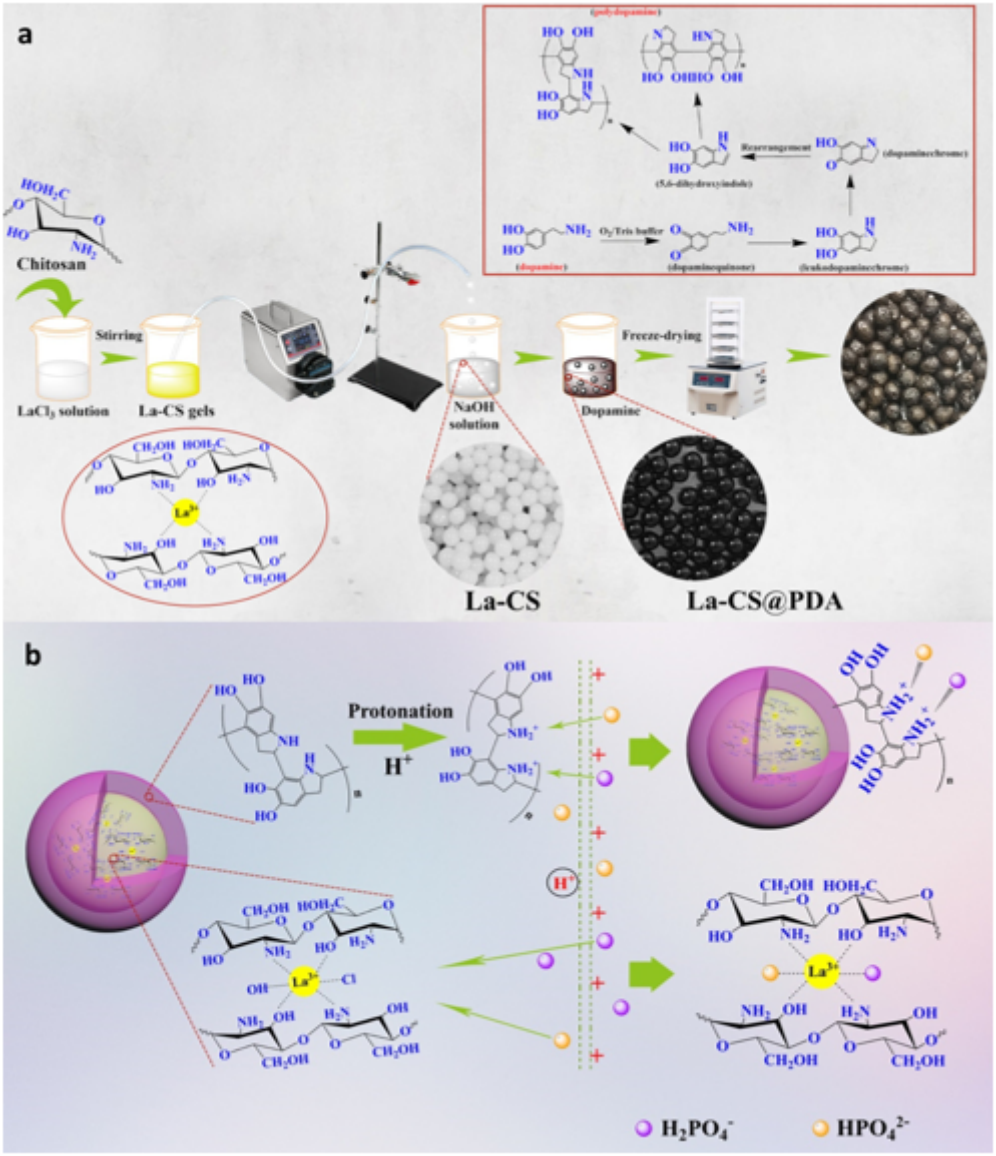

Figure 6

Preparation of La-CS@PDA beads (a) and proposed adsorption mechanism for phosphate (b) (Zhao et al. 2020). Copyright 2020. Reproduced with permission from Elsevier.

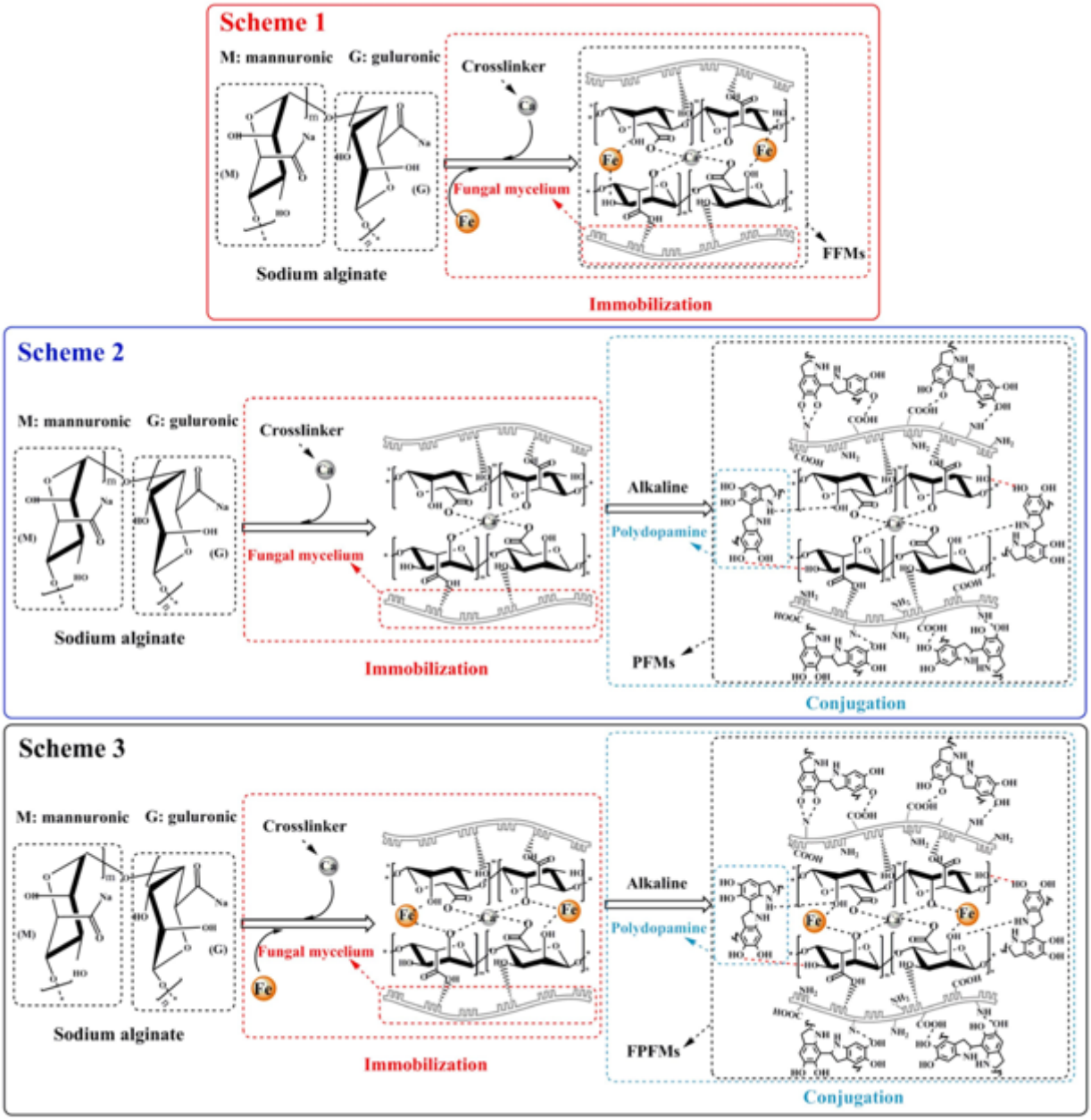

Figure 7

Preparation process of FFMs, PFMs and FPFMs adsorbents (Ding et al. 2019). Copyright 2019. Reproduced with permission from Elsevier.

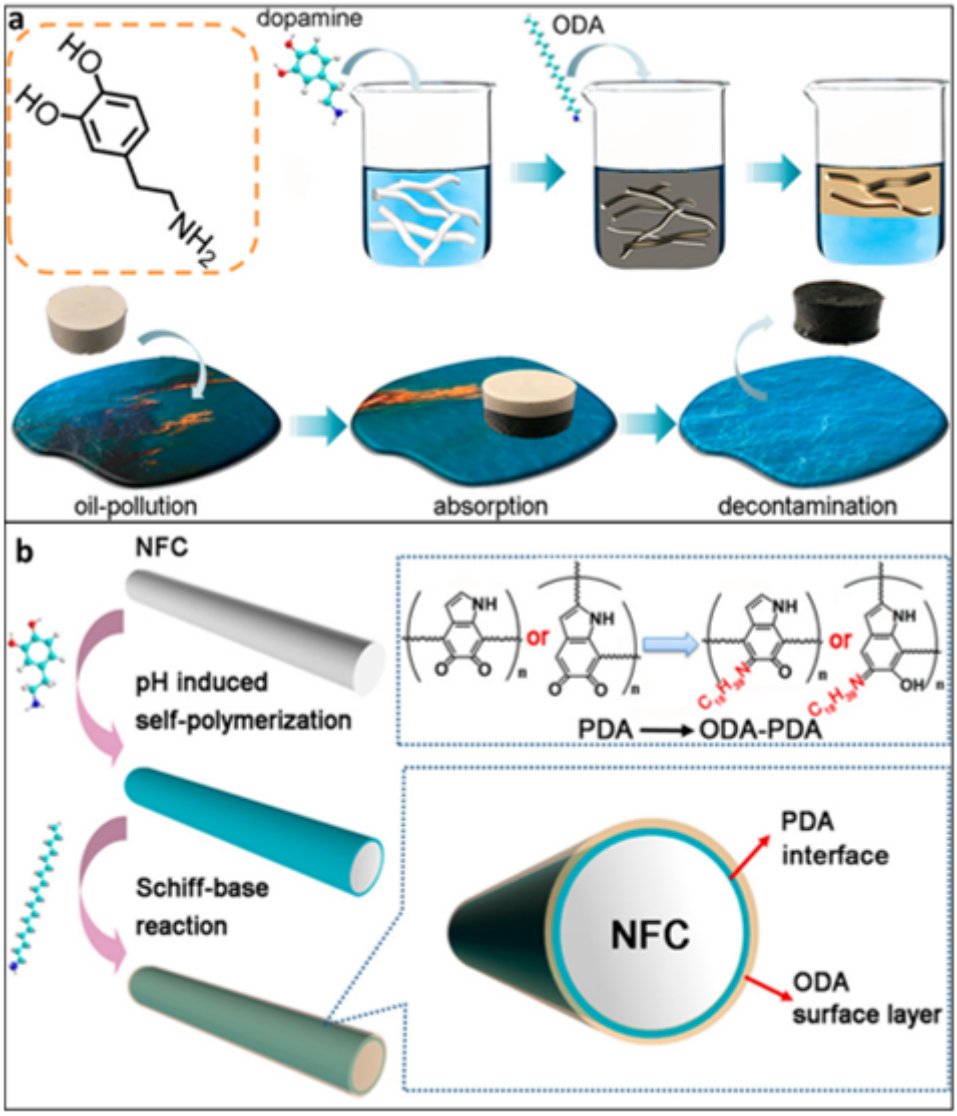

Figure 8

Preparation process (a) and mechanism (b) of NFC-based aerogels (Gao et al. 2018). Copyright 2018. Reproduced with permission from American Chemical Society.

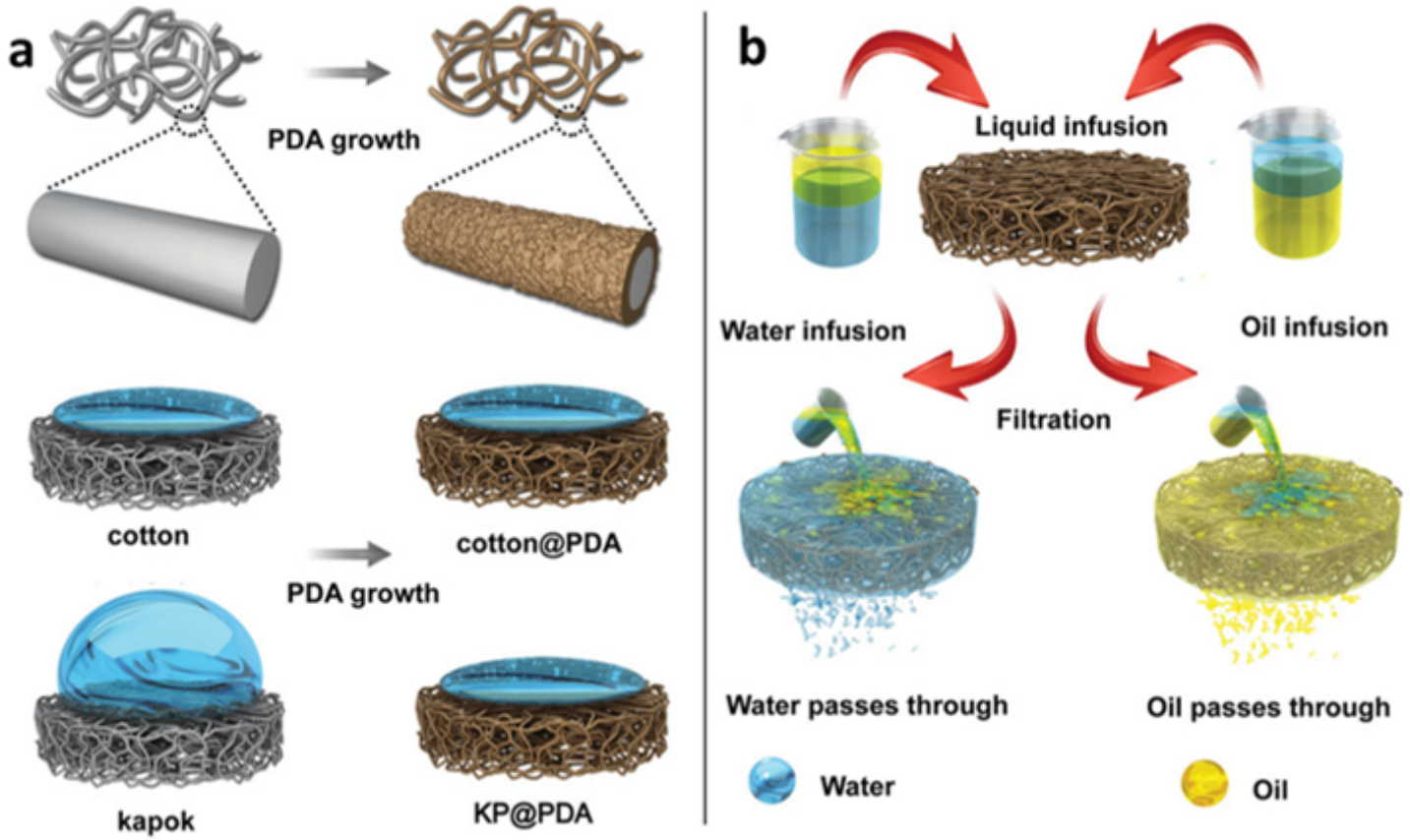

Figure 9

Preparation of PDA-functionalized membranes for oil-water separation (Mai et al. 2020). Copyright 2020. Reproduced with permission from JOHN WILEY & SONS.

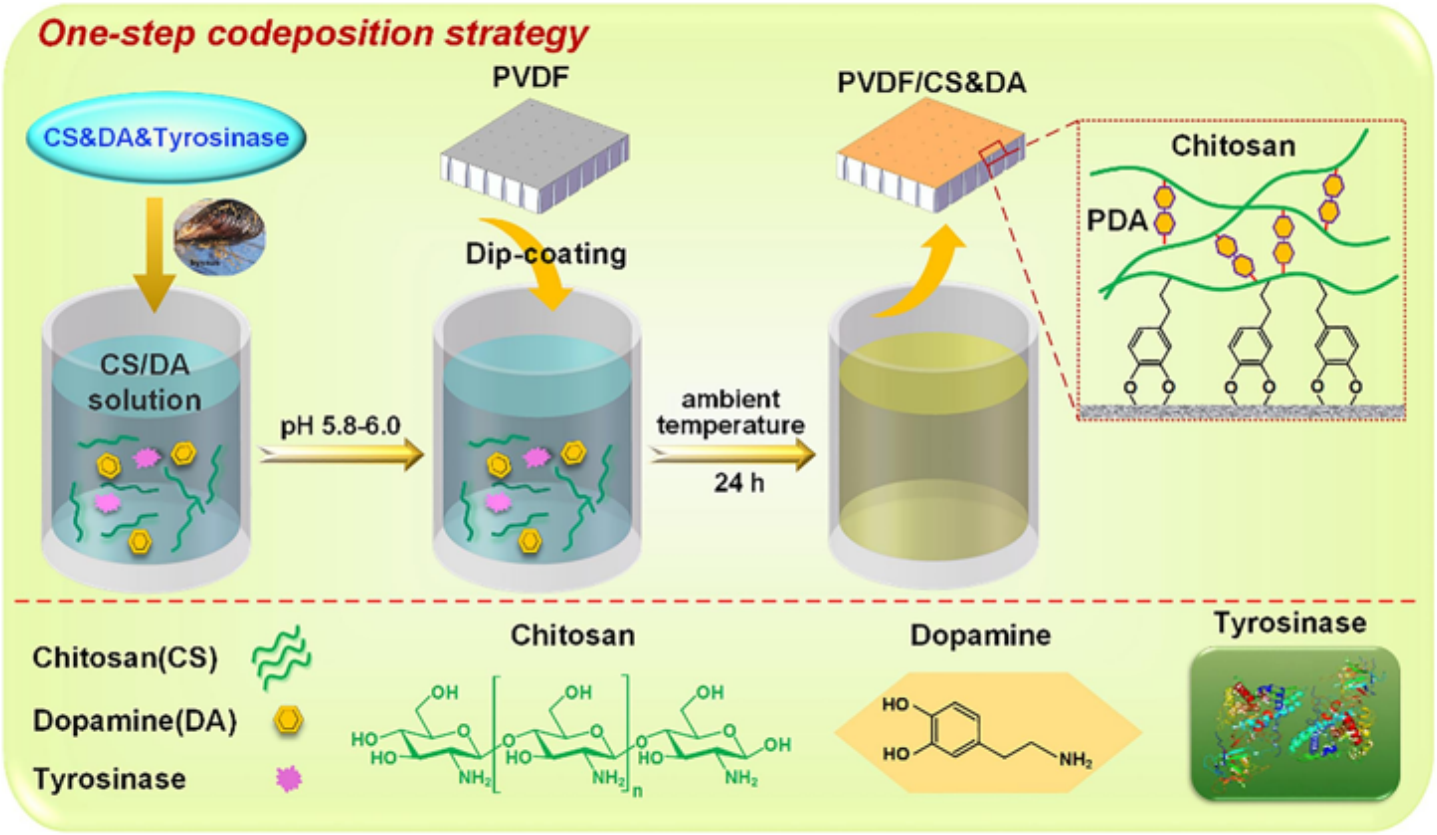

Figure 10

Preparation process of PVDF/CS&DA membranes (Zhang et al. 2019). Copyright 2019. Reproduced with permission from Elsevier.

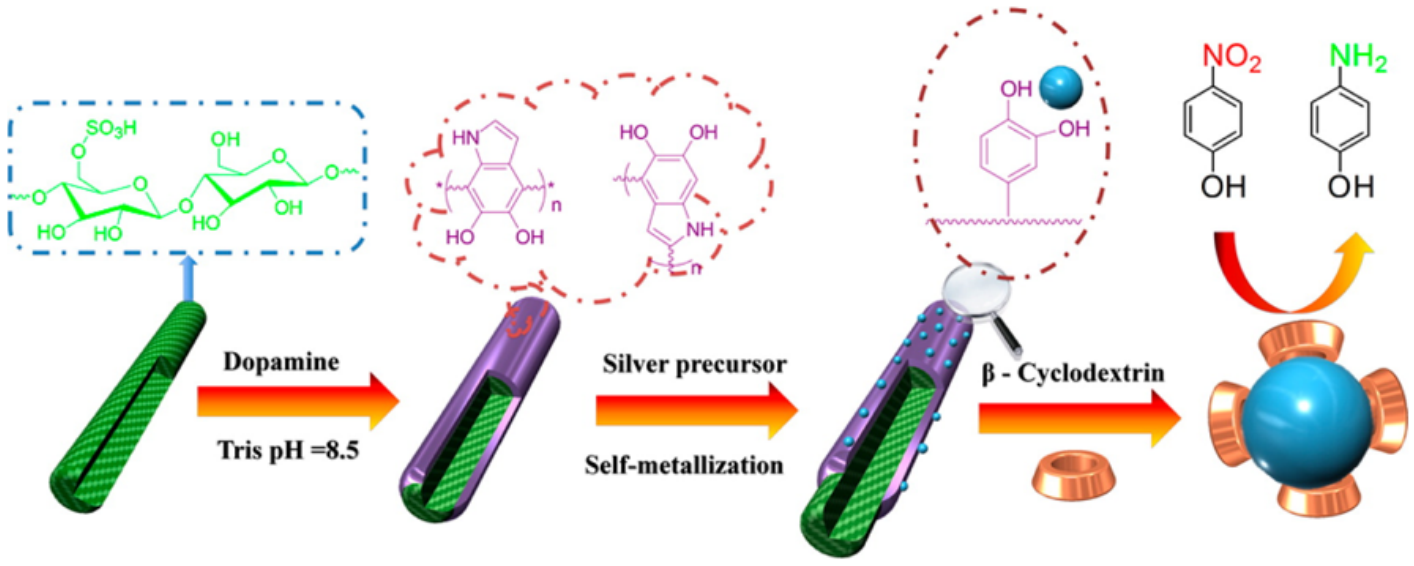

Figure 11

Preparation process of CNC@PDA (Tang et al. 2015). Copyright 2015. Reproduced with permission from American Chemical Society.

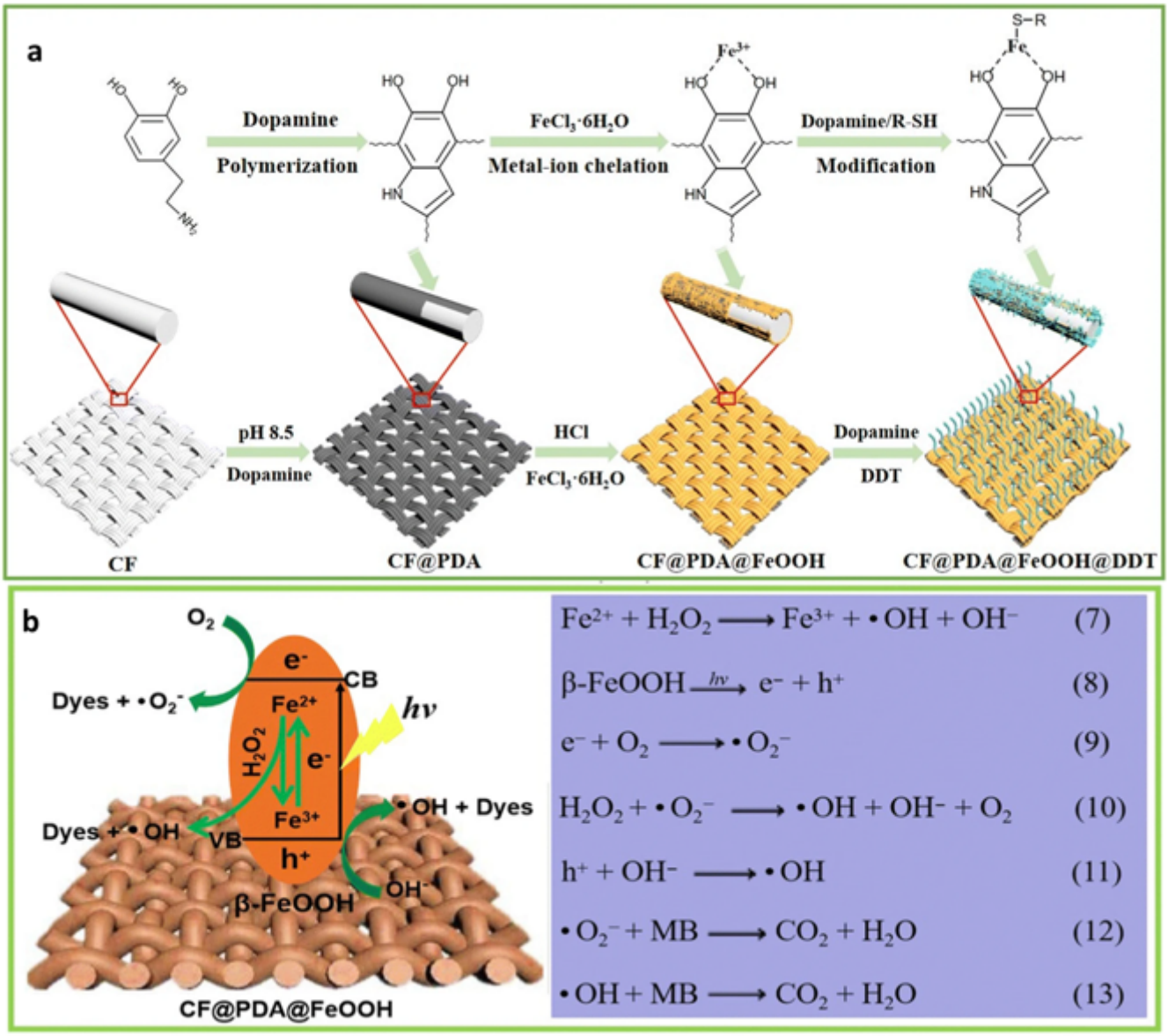

Figure 12

(a) Preparation process of superhydrophobic cotton fabric. (b) Possible photocatalytic mechanism (Cheng et al. 2020b). Copyright 2020. Reproduced with permission from Springer Nature.

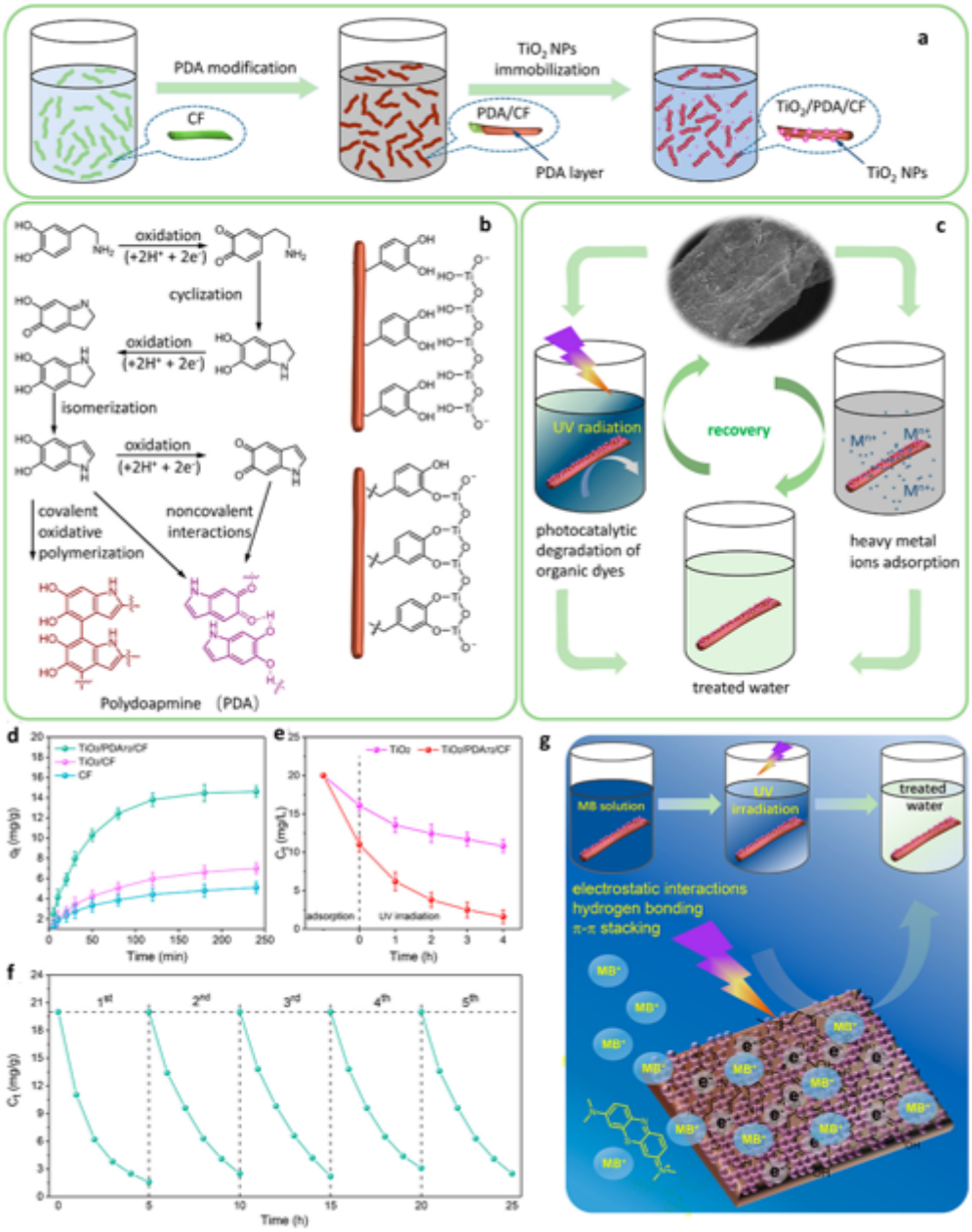

Figure 13

(a) Preparation process of PDA-coated cellulose-based nanocomposite fibers. (b) Formation mechanism. (c) Use for wastewater treatment. (d) Adsorption of MB. (e) Photocatalytic degradation property. (f) Recoverability. (g) Schematic diagram of photocatalytic degradation of MB (Liu et al. 2018). Copyright 2018. Reproduced with permission from American Chemical Society.

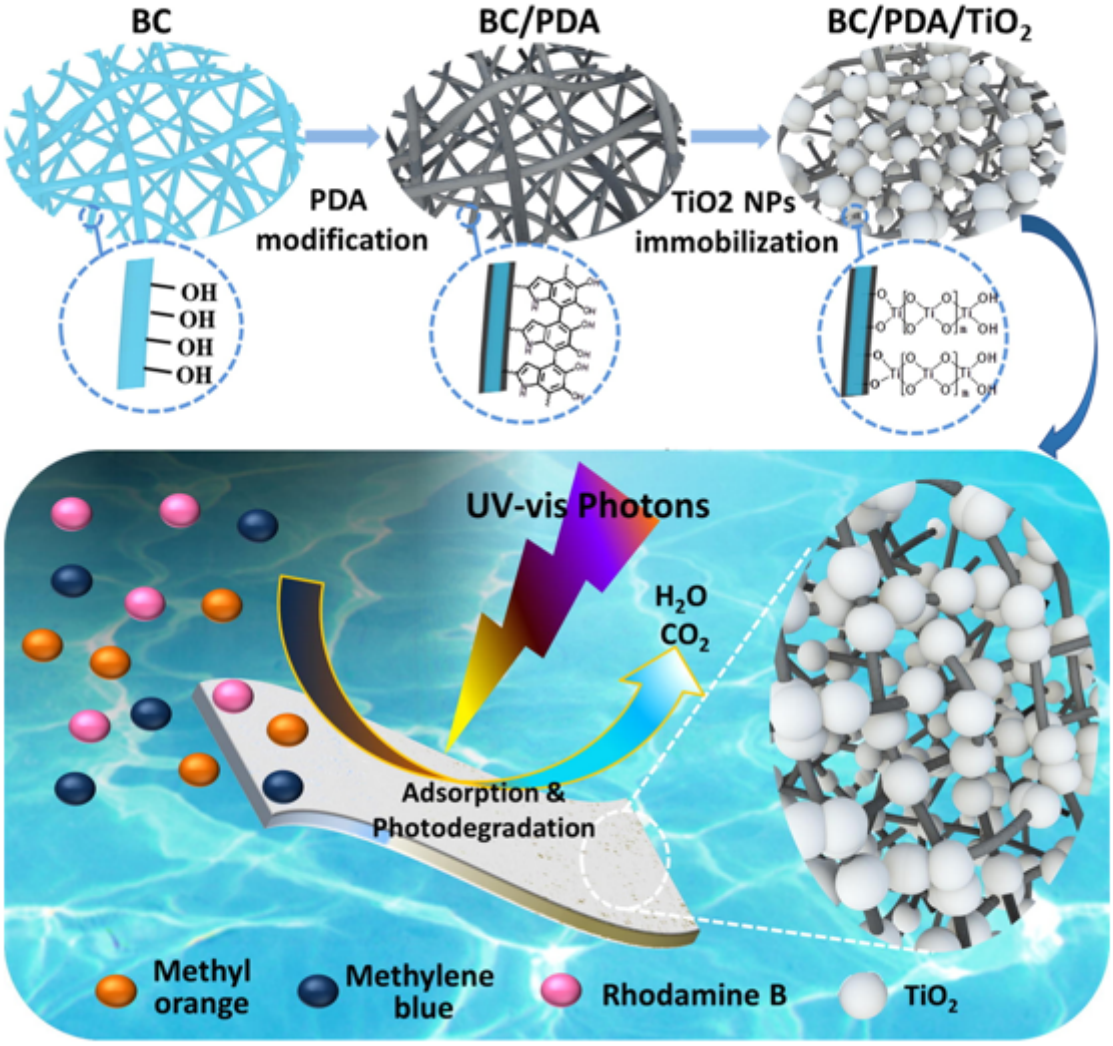

Figure 14

Fabrication of BC/PDA/TiO_2 nanocomposite membrane for the photocatalytic decomposition and adsorption of MO, MB and RB (Yang et al. 2020). Copyright 2020. Reproduced with permission from Elsevier.

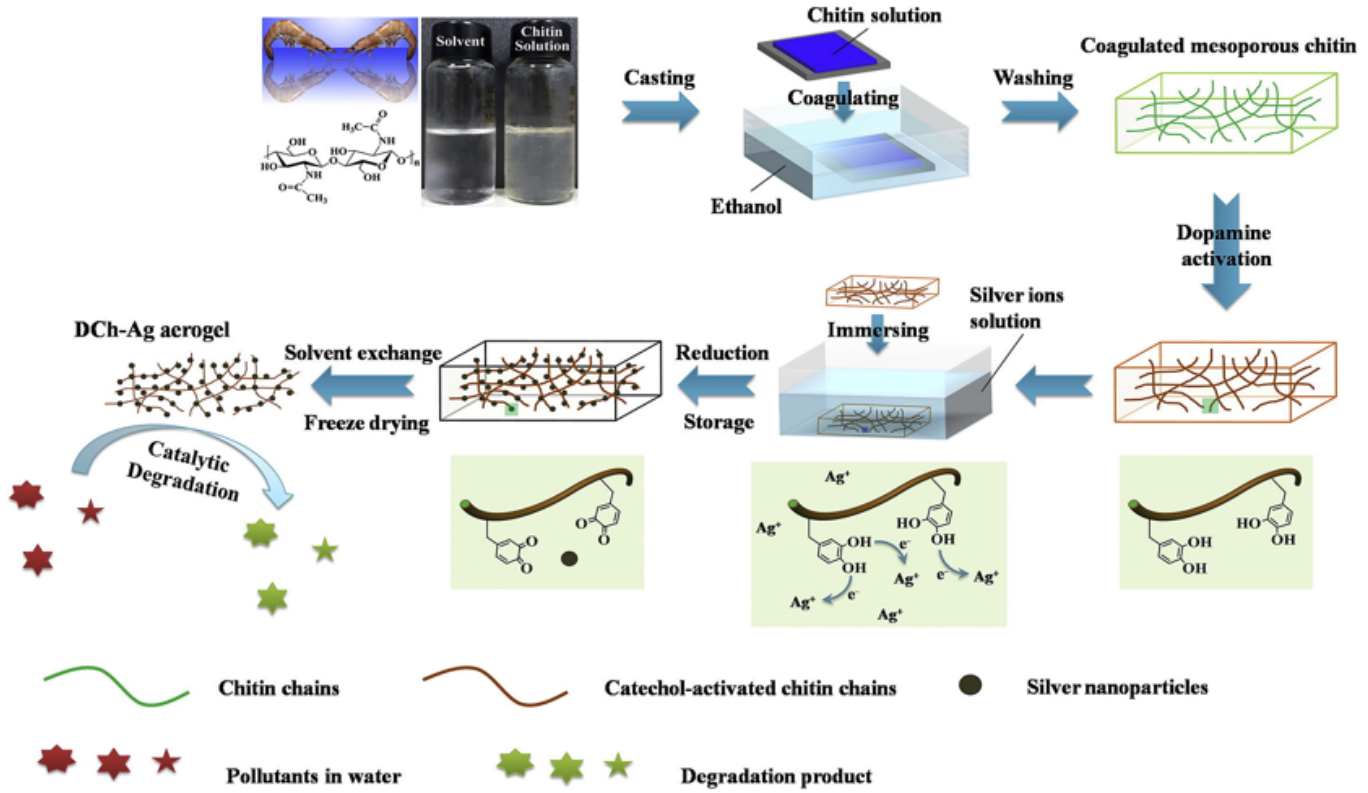

Figure 15

Preparation of chitin aerogel catalysts (Wang et al. 2017a). Copyright 2017. Reproduced with permission from Elsevier.

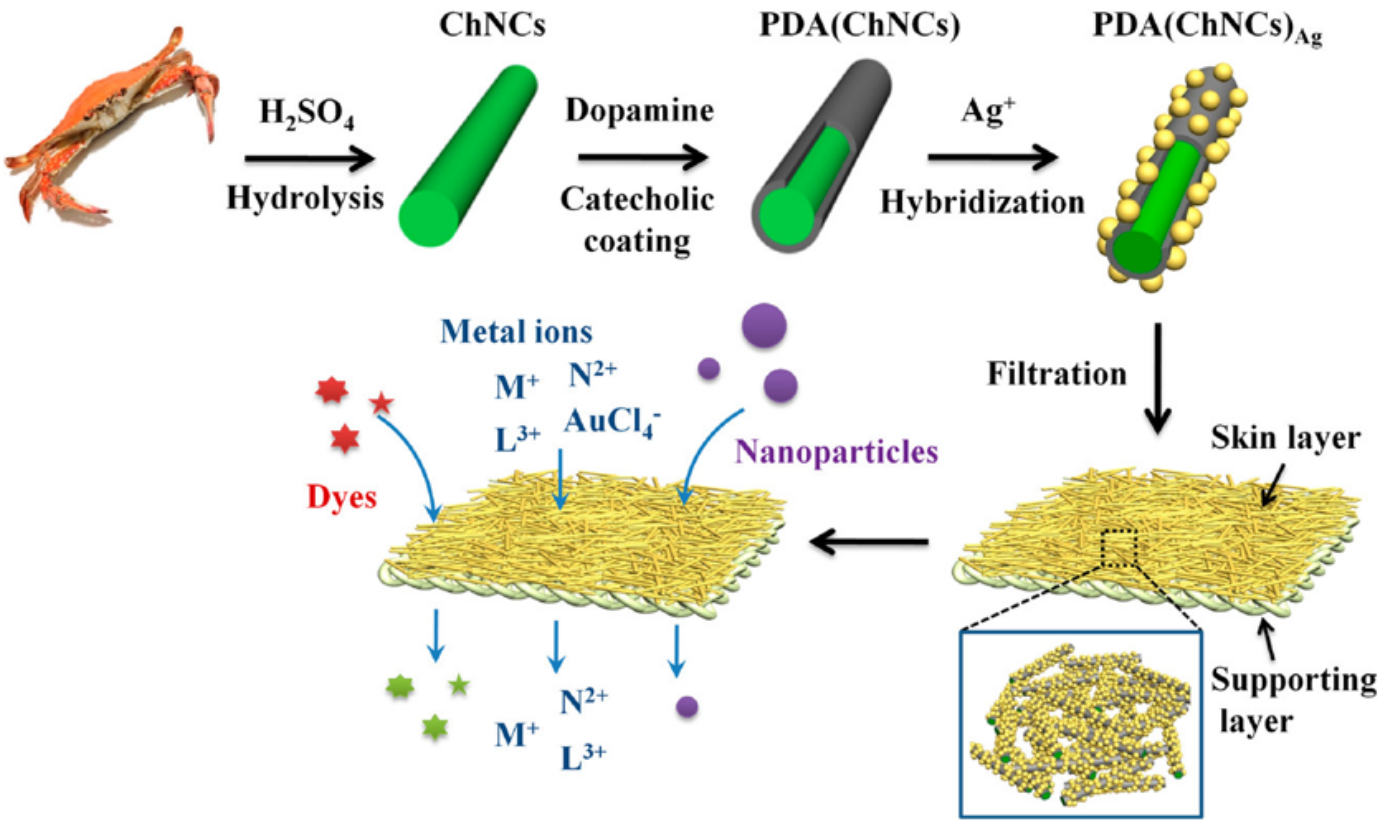

Figure 16

Preparation of hybrid AgNPs membranes (Wang et al. 2017b). Copyright 2017. Reproduced with permission from American Chemical Society.

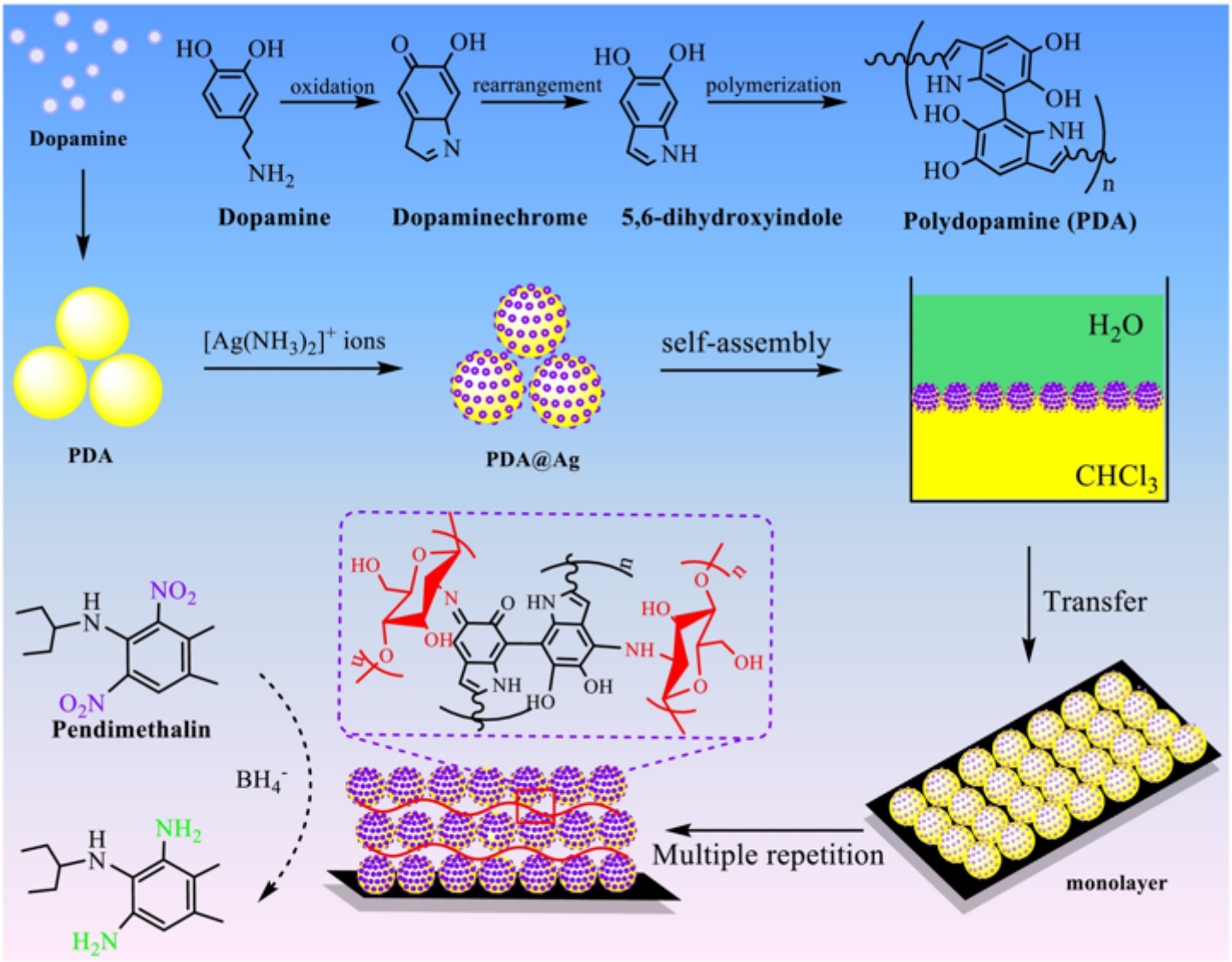

Figure 17

Preparation process of the PDA@Ag/PS/chitosan films and its catalytic degradation of pendimethalin (Xu et al. 2019). Copyright 2019. Reproduced with permission from Elsevier.

Figure 18

Fabrication of PDA-functionalized cellulose-based aerogel for solar-driven water remediation (Zhou et al. 2021). Copyright 2021. Reproduced with permission from American Chemical Society.

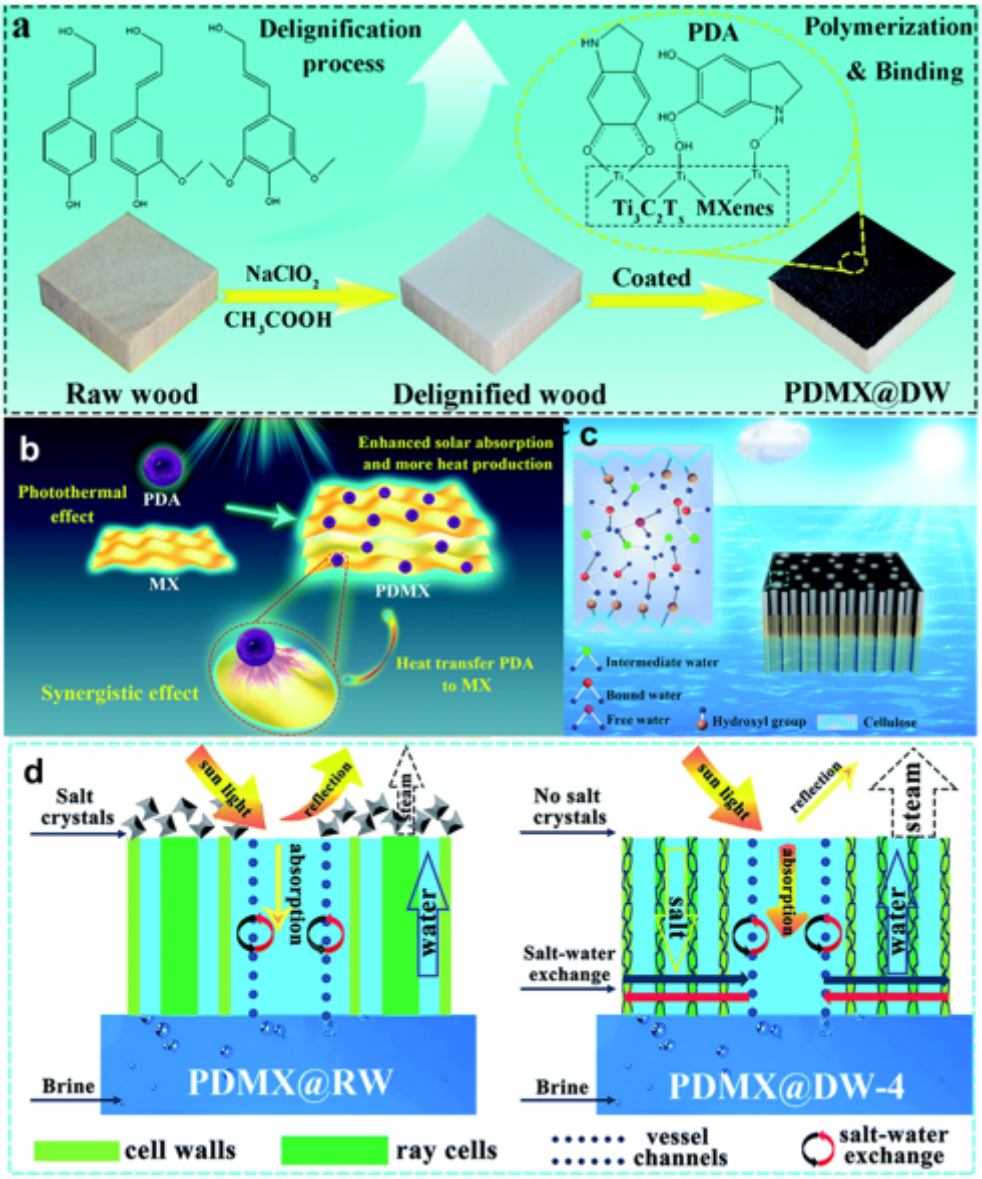

Figure 19

(a) Fabrication of PDA-functionalized cellulose-based evaporator. (b) Illustration of the synergistic photothermal effect. (c) Illustration of the evaporation mechanism. (d) Illustration of desalination process (Chen et al. 2021b). Copyright 2021. Reproduced with permission from Royal Society of Chemistry.

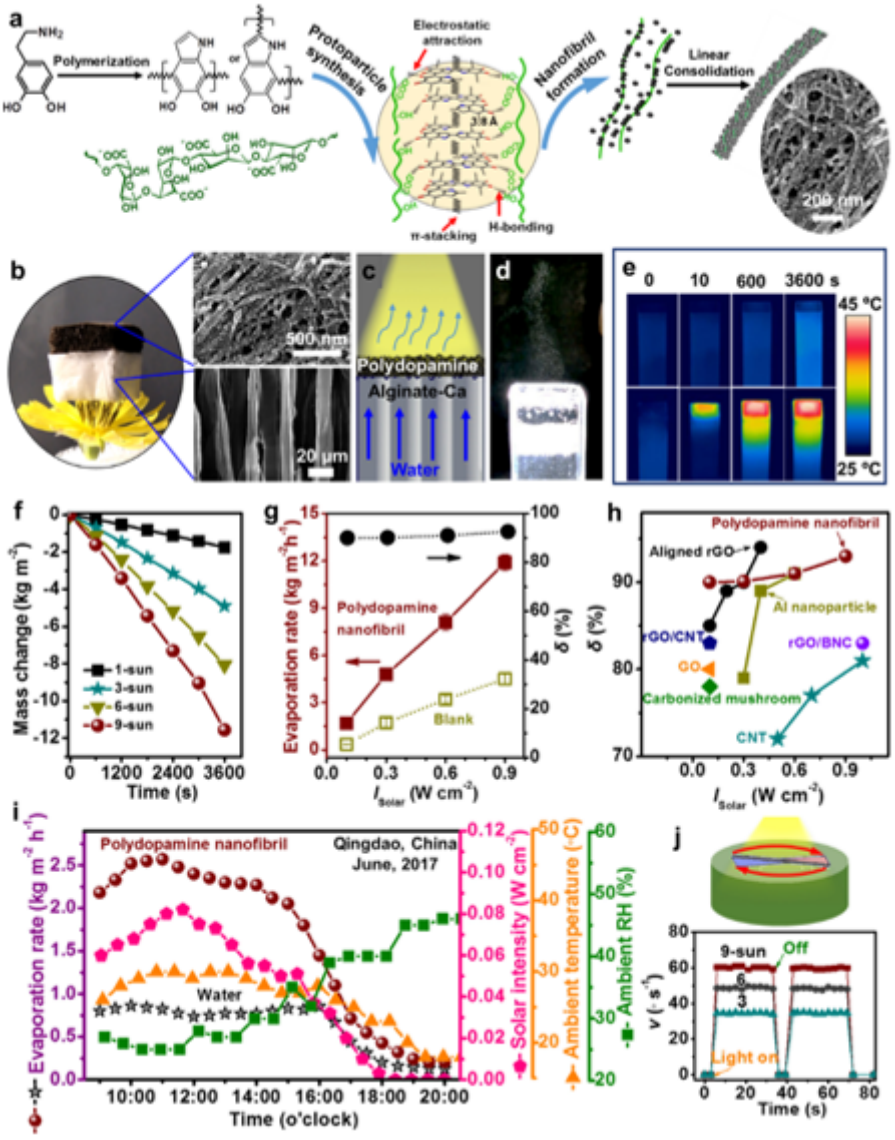

Figure 20

(a) Schematic diagram of preparation of PDA-functionalized alginate-based biologic nanostructures. (b) Photographs of nanofibril aerogel (top) supported on freeze-dried calcium alginate (bottom) and SEM images. (c) Schematic diagram of solar-thermal platform. (d) Photograph of the solar-thermal platform after six times of sun irradiation. (e) Infrared thermal pictures of nanofibril aerogel. (f) Mass changes of nanofibril aerogel. (g) Evaporation rate and δ values with the change of solar intensities. (h) δ values compared to diverse nanomaterials. (i) Solar steam generation ability outdoors. (j) A solar-driven rotator prepared by coating PDA nanofibrils on twisting polyvinylidene fluoride ribbon, showing diverse rotation speeds (v) under 3–9-sun irradiation (Zong et al. 2018). Copyright 2018. Reproduced with Elsevier.